

Toolkit for Scalar Fields in Universes with finite-dimensional Hilbert Space

Oliver Friedrich^{a,b} Ashmeet Singh^c Olivier Doré^d

^aFakultät für Physik, Ludwig-Maximilians Universität München,
Geschwister-Scholl-Platz 1, 80539 München, Germany

^bKavli Institute for Cosmology, University of Cambridge,
CB3 0HA Cambridge, United Kingdom

^cDepartment of Physics, California Institute of Technology,
1200 E. California Blvd., Pasadena, CA 91125, USA

^dJet Propulsion Laboratory, California Institute of Technology,
4800 Oak Grove Drive, Pasadena, CA 91109, USA

E-mail: oliver.friedrich@physik.lmu.de, ashmeet@caltech.edu,
olivier.p.dore@jpl.nasa.gov

Abstract. The holographic principle suggests that the Hilbert space of quantum gravity is locally finite-dimensional. Motivated by this point-of-view, and its application to the observable Universe, we introduce a set of numerical and conceptual tools to describe scalar fields with finite-dimensional Hilbert spaces, and to study their behaviour in expanding cosmological backgrounds. These tools include accurate approximations to compute the vacuum energy of a field mode \mathbf{k} as a function of the dimension $d_{\mathbf{k}}$ of the mode Hilbert space, as well as a parametric model for how that dimension varies with $|\mathbf{k}|$. We show that the maximum entropy of our construction momentarily scales like the boundary area of the observable Universe for some values of the parameters of that model. And we find that the maximum entropy generally follows a sub-volume scaling as long as $d_{\mathbf{k}}$ decreases with $|\mathbf{k}|$. We also demonstrate that the vacuum energy density of the finite-dimensional field is dynamical and decays between two constant epochs in our fiducial construction. These results rely on a number of non-trivial modelling choices, but our general framework may serve as a starting point for future investigations of the impact of finite-dimensionality of Hilbert space on cosmological physics.

Contents

1	Introduction	1
2	A finite-dimensional scalar field and its vacuum energy density	4
2.1	Infinite-dimensional scalar field in an expanding box	4
2.2	Finite-dimensional scalar field in an expanding box	6
2.3	Choice of IR scale	10
3	Increase in dimension and scaling of maximum entropy	11
4	Equation of state of finite-dimensional vacuum energy	13
4.1	Fiducial construction	13
4.2	Alternative choice of eigenvalue spacing	17
5	Summary of assumptions and discussion	20
A	Eigenvalue spacing that maximize vacuum energy	25
B	Approximating $E_{\min}(k)$	26
B.1	General case asymptotics	26
B.2	Expressions for late-time cosmology	28
C	Error function asymptotics, alternative construction	29

1 Introduction

The holographic principle [44, 46] states that the maximum entropy S that can be accumulated inside a finite region of space \mathcal{R} (with a sufficiently regular boundary $\delta\mathcal{R}$) equals the boundary area of that region divided by four times the Planck area [7, 45],

$$S(\mathcal{R}) \leq \frac{|\delta\mathcal{R}|}{4\ell_{\text{P}}^2}. \quad (1.1)$$

Since the maximum entropy that can be attained by a quantum system is proportional to the logarithm of the dimension of its Hilbert space, this can be interpreted such that the Hilbert space representing the region \mathcal{R} must be finite-dimensional [6, 11, 38]. This finite-dimensionality is a consequence of gravity: whereas quantum field theory without gravity has infinitely many degrees of freedom in any compact region of space, when we try to excite these degrees of freedom in the presence of gravity, many of the resulting states would collapse the region into a black hole. And black holes have a finite amount of entropy which scales as the area of their horizon. Therefore, any attempts to increase the region's entropy by creating further excitations would only increase the size of the resulting black hole, and hence the size of its supporting region, suggesting that the amount of entropy that can be localized in a compact region of space is finite [3, 4, 6, 14, 22, 23, 40, 50]. This argument based on local Hilbert space factors is oversimplified insofar as gauge theories typically do not permit spatial regions to be identified with unique Hilbert space factors [16, 20, 21, 25] (and

references therein), and the more precise statement would be that the observables associated with a finite region of space should have support in only a finite-dimensional Hilbert space factor. This interpretation of the holographic principle asserts a local finite-dimensionality of Hilbert space, and it can be extended to the entire (observable) cosmos by noting that in an asymptotically de-Sitter Universe the causal patch of any observer has a finite extent [2, 22]. Invoking observer complementarity, this means that the physics experienced by any observer in our Universe should be described by a finite-dimensional quantum theory [22, 39].

If this reasoning is correct, then no quantum field theory based on a non-compact symmetry group (including any group with local Lorentz symmetry) can be a fundamental description of physics in our Universe [6, 38] because all unitary representations of such groups live on infinite-dimensional Hilbert spaces. This also precludes conjugate variables which satisfy Heisenberg’s canonical commutation relation (CCR; and its extensions to field theory) since the latter can only be realized on an infinite-dimensional Hilbert space. Motivated by the lack of finite-dimensional representations of conjugate operators satisfying the CCR, [42] have used generalised Pauli operators (GPOs) as a framework to construct finite-dimensional analogs of conjugate Hermitian operators. These operators were then used by [11] to build a finite-dimensional version of a scalar quantum field. They also demonstrated that the zero-point energy of such fields is significantly reduced wrt. infinite-dimensional counterparts. This hints at potentially observable consequences of finite-dimensionality for quantum fields even when a fixed background spacetime is assumed.

Ultimately, notions of space and spacetime symmetries may be emergent phenomena of an underlying, purely quantum theory [9, 10, 13, 14, 18, 22, 26, 47], in which case it would not be surprising that familiar symmetry groups are not fundamental. According to [15], quantum fields would then only be effective descriptions of emergent pointer observables which in turn result from emergent system-environment splits that maximise notions of locality, predictability and robustness against decoherence [see also 18, for related thoughts]. It remains a challenge for this “quantum first” program to construct concrete models (of e.g. cosmological physics) that incorporate these concepts of emergence. We think that the approach of [42] and [11] for constructing finite-dimensional quantum fields can be a fruitful starting point for the development of such models [see e.g. 5, 12, for different approaches].

In this paper, we revisit the framework of generalized Pauli operators to construct a finite-dimensional rendering of a scalar field and develop the following extensions, with an eye toward cosmological applications:

- i. We develop a finite-dimensional model of scalar field dynamics in a flat Friedmann-Lemaître-Robertson-Walker (FLRW) spacetime.
- ii. We investigate two distinct choices for the eigenvalue spacings of the finite-dimensional field operators. In our fiducial construction, we choose those spacings in a way that *minimizes* finite-dimensional effects on the ground state energy of the field. We also show that the variance of the scalar field and the variance of its canonically conjugate momentum field in the ground state are equally well resolved with our choice of eigenvalue spacing. Both of these properties ensure that - in the ground state - our construction closely resembles the infinite-dimensional limit (which is also a prerequisite for the emergence of classicality in low energy physics).
- iii. In an alternative construction, we choose the eigenvalue spacing of the finite-dimensional field operators in a way that ensures an algebraic symmetry between the field and its

conjugate momentum. We show that in this case the effect of finite-dimensionality on the energy eigenspectrum is drastically increased.

- iv. We derive accurate approximations for the ground state energy of the finite-dimensional harmonic oscillator as a function of frequency and the dimension of its Hilbert space. These approximations are numerically feasible for arbitrarily high dimension and agree with the exact calculation of [42] to better than 3% accuracy for dimensions ≥ 7 .
- v. We introduce a parametric model for how the dimension $d_{\mathbf{k}}$ of the Hilbert space corresponding to the co-moving mode \mathbf{k} of our field depends on $|\mathbf{k}|$. While that model is likely to be overly simplistic, it allows us to qualitatively study how consistency with low energy physics can constrain its parameter space, and how different parameter values impact the behaviour of the finite-dimensional field. For example, we find that the maximum entropy attainable with our construction follows a sub-volume scaling with the size of the observable Universe as long as $d_{\mathbf{k}}$ is a decreasing function of $|\mathbf{k}|$, and that it can momentarily even display an area-scaling.
- vi. We study the equation of state of the vacuum energy density of the finite-dimensional scalar field as a function of the dimensionality parameters. For much of the allowed parameter space that energy density becomes dynamical. With our fiducial choice for the eigenvalue spacing of the conjugate field operators it is decaying between two constant epochs with an asymptotic suppression of vacuum energy by about 40%. For our alternative choice of the eigenvalue spacing it is decaying indefinitely, easily reaching a $\sim 10^{-60}$ suppression compared to the infinite-dimensional calculation (with sharp UV cut-off) for some parameter values.

We have implemented the above framework within the `GPUuniverse` toolkit that is publicly available at <https://github.com/OliverFHD/GPUuniverse>. Our paper is structured as follows: In Section 2, we construct our finite-dimensional version of the scalar field in an expanding universe and derive expressions for its vacuum energy density, with the derivation of some key statements outsourced to Appendices A and B. In Section 3, we investigate how the number of degrees of freedom in our field scale with the size of the universe, and we discuss a potential interpretation of that dynamical increase of Hilbert space dimension within the context of the work of [5]. In Section 4, we study the equation of state of vacuum energy density of the finite-dimensional scalar field as a function of the parameters describing how the dimension of individual mode Hilbert spaces depends on the absolute value $|\mathbf{k}|$ of those modes (cf. point v. above). We also derive there a number of consistency requirements for those dimensionality parameters, and we investigate how the behaviour of vacuum energy density changes if we switch from our fiducial eigenvalue spacing of the field operators (cf. point ii. above) to the alternative choice (cf. point iii.). In Section 5, we discuss the assumptions and limitations of our construction as well as possible directions for future investigation. Throughout this paper we are working with natural units, i.e. we put $\hbar = G = c = 1$, unless stated otherwise.

2 A finite-dimensional scalar field and its vacuum energy density

2.1 Infinite-dimensional scalar field in an expanding box

Let us first recap the conventional, infinite-dimensional construction of a real scalar field on a curved spacetime, with the action

$$S = \frac{1}{2} \int \sqrt{-g} d^4x \left[g^{\alpha\beta} \phi_{,\alpha} \phi_{,\beta} - m^2 \phi^2 \right], \quad (2.1)$$

where g is the determinant, and $g^{\alpha\beta}$ are the components of the inverse of the metric tensor. In a flat Friedmann universe, and using the conformal form of the metric

$$ds^2 = a^2 (d\eta^2 - d\mathbf{x}^2), \quad [\cdot]' \equiv \frac{\partial}{\partial \eta}[\cdot], \quad (2.2)$$

this becomes

$$\begin{aligned} S &= \frac{1}{2} \int d\eta d^3x \, a^2 \left[(\phi')^2 - (\nabla\phi)^2 - m^2 a^2 \phi^2 \right] \\ &= \frac{1}{2} \int \frac{d\eta d^3k}{(2\pi)^3} \, a^2 \left[|\phi'_{\mathbf{k}}|^2 - (|\mathbf{k}|^2 + m^2 a^2) |\phi_{\mathbf{k}}|^2 \right], \end{aligned} \quad (2.3)$$

where in the second line we moved to Fourier space, with \mathbf{k} labeling a co-moving Fourier mode. Expressing the Fourier transform of the field in terms of real and imaginary parts, $\phi_{\mathbf{k}} = A_{\mathbf{k}} + iB_{\mathbf{k}}$, we must have $A_{\mathbf{k}} = A_{-\mathbf{k}}$ and $B_{\mathbf{k}} = -B_{-\mathbf{k}}$ because ϕ is real. This allows us to define a new field

$$q_{\mathbf{k}} = \sqrt{2} \begin{cases} A_{\mathbf{k}} & \text{for } k_1 \leq 0 \\ B_{\mathbf{k}} & \text{for } k_1 > 0 \end{cases} \quad (2.4)$$

such that the action can be re-written as [37]

$$S = \int \frac{d\eta d^3k}{(2\pi)^3} \left[\frac{a^2}{2} (q'_{\mathbf{k}})^2 - \frac{a^2 (|\mathbf{k}|^2 + m^2 a^2)}{2} q_{\mathbf{k}}^2 \right]. \quad (2.5)$$

This can be interpreted as an action corresponding to a collection harmonic oscillators with time dependent mass a^2 and time dependent frequency $\sqrt{|\mathbf{k}|^2 + m^2 a^2}$ [36, 37]. To make this analogy more explicit, let us restrict the field ϕ to a finite box of co-moving side length L_c , imposing periodic boundary conditions. This modifies the action to

$$S_{\text{box}} = \int d\eta \frac{1}{L_c^3} \sum_{\mathbf{k}} \left[\frac{a^2}{2} (q'_{\mathbf{k}})^2 - \frac{a^2 (|\mathbf{k}|^2 + m^2 a^2)}{2} q_{\mathbf{k}}^2 \right], \quad (2.6)$$

where we have use the fact that $d^3k \rightarrow \Delta k^3 = (2\pi/L_c)^3$ and the sum is over all $\mathbf{k} = (k_1, k_2, k_3)$ with $k_i \in \{2\pi n/L_c \mid n \in \mathbb{Z}\}$. In order to extract the Hamiltonian from that action, let us re-write it in terms of physical time $dt = a d\eta$, i.e.

$$S_{\text{box}} = \int dt \frac{a^3}{L_c^3} \sum_{\mathbf{k}} \left[\frac{1}{2} (\dot{q}_{\mathbf{k}})^2 - \frac{(|\mathbf{k}|^2/a^2 + m^2)}{2} q_{\mathbf{k}}^2 \right] \equiv \int dt L_{\text{box}}(\{q_{\mathbf{k}}\}, \{\dot{q}_{\mathbf{k}}\}, t). \quad (2.7)$$

Here the last equality serves as a definition of the Lagrangian L_{box} of the discretized field. It is literally the Lagrangian of a set of harmonic oscillators with masses a^3/L_c^3 and frequencies $\sqrt{|\mathbf{k}|^2/a^2 + m^2}$. The corresponding Hamiltonian is given by

$$H_{\text{box}}(\{q_{\mathbf{k}}\}, \{p_{\mathbf{k}}\}, t) = \sum_{\mathbf{k}} \left[\frac{L_c^3}{2a^3} p_{\mathbf{k}}^2 + \frac{a^3}{L_c^3} \frac{(|\mathbf{k}|^2/a^2 + m^2)}{2} q_{\mathbf{k}}^2 \right], \quad (2.8)$$

where we introduced the conjugate momenta $p_{\mathbf{k}} = \partial L_{\text{box}}/\partial \dot{q}_{\mathbf{k}}$. To obtain the quantum theory of this field one would usually promote $q_{\mathbf{k}}$ and $p_{\mathbf{k}}$ to conjugate Hermitian operators satisfying the Heisenberg commutation relations

$$[\hat{q}_{\mathbf{k}}, \hat{p}_{\mathbf{k}'}] = i\delta_{\mathbf{k}, \mathbf{k}'} \quad (2.9)$$

such that the Hamiltonian operator of the field becomes

$$\hat{H}(t) = \sum_{\mathbf{k}} \left[\frac{L_c^3}{2a^3} \hat{p}_{\mathbf{k}}^2 + \frac{a^3}{L_c^3} \frac{(|\mathbf{k}|^2/a^2 + m^2)}{2} \hat{q}_{\mathbf{k}}^2 \right]. \quad (2.10)$$

which at any time t has the minimum eigenvalue

$$\lambda_{\min} [\hat{H}(t)] = \frac{1}{a} \sum_{|\mathbf{k}| < k_{\max}} \frac{\sqrt{|\mathbf{k}|^2 + m^2 a^2}}{2}. \quad (2.11)$$

Here we have introduced a co-moving ultra-violet cut-off k_{\max} in order to regularise this otherwise divergent expression. Such a sharp cut-off has been criticized because it breaks Lorentz symmetry [1, 34]. There are however reasons to believe that the breaking of Lorentz symmetry is physical [6, 27, 35], including the premise of this paper: finite-dimensionality of Hilbert space.

To obtain the vacuum energy density of the field we need to divide this eigenvalue by the physical volume of the box, i.e. by

$$V_{\text{ph}} = L_{\text{ph}}^3 \equiv (aL_c)^3, \quad (2.12)$$

where $L_{\text{ph}} = aL$ is the physical box size. The energy density of the vacuum is then given by

$$\epsilon_{\text{vac}} = \frac{1}{a^4 L_c^3} \sum_{|\mathbf{k}| < k_{\max}} \frac{\sqrt{|\mathbf{k}|^2 + m^2 a^2}}{2}. \quad (2.13)$$

For a constant co-moving box size L_c this seems to indicate that $\epsilon_{\text{vac}} \propto a^{-4}$, which is the behaviour of a relativistic fluid, and not that of a cosmological constant. However, it is usually assumed that the scale regularising a QFT is some fix *physical* scale Λ_{UV} , which for the rest of this paper we will take to be equal to the Planck mass. In an expanding Universe we would then have $k_{\max} = a\Lambda_{\text{UV}}$, such that Equation 2.13 becomes

$$\epsilon_{\text{vac}} = \frac{1}{a^4 L_c^3} \sum_{|\mathbf{k}| < a\Lambda_{\text{UV}}} \frac{\sqrt{|\mathbf{k}|^2 + m^2 a^2}}{2}. \quad (2.14)$$

For $\Lambda_{\text{UV}} \gg m$ the sum in this expression is proportional to a^4 , so that ϵ_{vac} is indeed constant. This is still somewhat curious, because a direct calculation of the vacuum pressure p_{vac}

from the vacuum stress-energy tensor yields $p_{\text{vac}} \approx \epsilon_{\text{vac}}/3$ [1], which is again the behaviour of a relativistic fluid. Note however, that the number of modes \mathbf{k} over which we sum in Equation 2.14 is now itself a function of time, and that this compensates for the energy loss that a relativistic fluid would experience in an expanding universe [35, 43]. This can be interpreted in terms of a modified continuity equation for the vacuum energy density [43].

We want to stress an important subtlety: Since the Hamiltonian in Equation 2.10 is time dependent, it is not possible for the field to remain in a state of minimum energy. Instead, each of the $q_{\mathbf{k}}$ behaves as a driven harmonic oscillator and the expansion of the Universe will inevitably lead to particle production [36, 37]. If the period of the oscillators around the cut-off Λ_{UV} is much smaller than the characteristic time scales over which a changes, then particle production will be negligible and the quantum state will undergo adiabatic evolution, i.e., stay in the instantaneous minimum energy eigenstate to a good approximation as time evolves. We will employ this adiabaticity assumption for the remainder of this paper. The assumption is well justified in late-time cosmology because the time scales relevant for the recent cosmic expansion history are much longer than the period of any cut-off scale that is relevant to well understood particle physics.

2.2 Finite-dimensional scalar field in an expanding box

We now return to our premise that the dimension of the Hilbert space of the observable Universe should be finite. In this case, the dimensions of the Hilbert spaces corresponding to individual modes \mathbf{k} also need to be finite. In the conventional infinite-dimensional setting, such as non-relativistic quantum mechanics of a single particle, classical conjugate variables \hat{q} and \hat{p} are promoted to Hermitian Hilbert space operators which obey the Heisenberg canonical commutation relation (CCR)

$$[\hat{q}, \hat{p}] = i, \quad (2.15)$$

where we have set $\hbar = 1$. In a quantum field theory, the field and its conjugate momentum are operator-valued functions on spacetime which obey a continuous version of the CCR, labelled by the field modes, as done in the previous section. The Stone-von Neumann theorem guarantees that there is an irreducible representation of the CCR, which is unique up to unitary equivalence, on any infinite-dimensional Hilbert space that is separable (i.e., that possesses a countable dense subset) [33]. However, in this case, the theorem also implies that the operators $\hat{\phi}$ and $\hat{\pi}$ must be unbounded. There are therefore no irreducible representations of Equation 2.9 on finite-dimensional Hilbert spaces, and one needs to consider a more general algebraic structure than the one imposed by Heisenberg's CCR.

Before we switch to a finite-dimensional construction, let us define convenient, dimensionless versions of our conjugate variables as

$$Q_{\mathbf{k}} \equiv q_{\mathbf{k}}/L_c^2, \quad P_{\mathbf{k}} \equiv p_{\mathbf{k}}L_c^2. \quad (2.16)$$

We would like to promote these to finite-dimensional, hermitian operators $\hat{Q}_{\mathbf{k}}, \hat{P}_{\mathbf{k}}$ that still allow for the emergence of semi-classical physics in the infinite-dimensional limit. In order to achieve this we follow the ansatz of [11, 42] and model $\hat{Q}_{\mathbf{k}}, \hat{P}_{\mathbf{k}}$ in terms of generalized Pauli operators $\hat{A}_{\mathbf{k}}, \hat{B}_{\mathbf{k}}$ (GPOs) as

$$\hat{A}_{\mathbf{k}} = \exp\left(-i\alpha_{\mathbf{k}}\hat{P}_{\mathbf{k}}\right), \quad \hat{B}_{\mathbf{k}} = \exp\left(i\beta_{\mathbf{k}}\hat{Q}_{\mathbf{k}}\right), \quad (2.17)$$

which are defined on a Hilbert space of finite dimension $d_{\mathbf{k}}$ and satisfy the Weyl commutation relation [49]

$$\hat{A}_{\mathbf{k}}\hat{B}_{\mathbf{k}} = \exp\left(\frac{-2\pi i}{d_{\mathbf{k}}}\right)\hat{B}_{\mathbf{k}}\hat{A}_{\mathbf{k}}, \quad (2.18)$$

and the closure property $\hat{A}_{\mathbf{k}}^{d_{\mathbf{k}}} = \mathbb{I}_{d_{\mathbf{k}}} = \hat{B}_{\mathbf{k}}^{d_{\mathbf{k}}}$, where $\mathbb{I}_{d_{\mathbf{k}}}$ is the identity operator on the Hilbert space of dimension $d_{\mathbf{k}}$. Equation 2.18 above is an exponentiated form of Heisenberg's CCR in the sense that when the real parameters, $\alpha_{\mathbf{k}}$ and $\beta_{\mathbf{k}}$ satisfy

$$\alpha_{\mathbf{k}}\beta_{\mathbf{k}} = \frac{2\pi}{d_{\mathbf{k}}}, \quad (2.19)$$

then Equation 2.18 is equivalent to Equation 2.9 in the limit $d_{\mathbf{k}} \rightarrow \infty$. The operators $\hat{Q}_{\mathbf{k}}$ and $\hat{P}_{\mathbf{k}}$ defined through Equations 2.17 and 2.18 do indeed admit a unitary representation on a Hilbert space with finite dimension $d_{\mathbf{k}}$. Moreover, the representation is still unique up to unitary equivalence via the Stone-von Neumann theorem, since a finite-dimensional Hilbert space is separable. For example, let the dimension of Hilbert space be $d_{\mathbf{k}} = 2\ell_{\mathbf{k}} + 1$ for some non-negative integer $\ell_{\mathbf{k}}$. Then the GPOs have the following matrix representation (up to unitary equivalence)

$$\hat{A}_{\mathbf{k}} = \begin{pmatrix} 0 & 0 & 0 & \cdots & 0 & 1 \\ 1 & 0 & 0 & \cdots & 0 & 0 \\ 0 & 1 & 0 & \cdots & 0 & 0 \\ \vdots & \vdots & \vdots & \ddots & \vdots & \vdots \\ 0 & 0 & 0 & \cdots & 0 & 0 \\ 0 & 0 & 0 & \cdots & 1 & 0 \end{pmatrix}_{d_{\mathbf{k}} \times d_{\mathbf{k}}}, \quad \hat{B}_{\mathbf{k}} = \begin{pmatrix} \exp(\frac{2\pi i}{d_{\mathbf{k}}}\ell_{\mathbf{k}}) & 0 & \cdots & 0 \\ 0 & \exp(\frac{2\pi i}{d_{\mathbf{k}}}(\ell_{\mathbf{k}} - 1)) & \cdots & 0 \\ \vdots & \vdots & \ddots & \vdots \\ 0 & 0 & \cdots & \exp(\frac{-2\pi i}{d_{\mathbf{k}}}\ell_{\mathbf{k}}) \end{pmatrix}_{d_{\mathbf{k}} \times d_{\mathbf{k}}}, \quad (2.20)$$

which indeed satisfy Equation 2.18. The construction works for even dimensions as well, but we focus on odd values to streamline the notation. It can then be shown [42] that the operators $\hat{Q}_{\mathbf{k}}$ and $\hat{P}_{\mathbf{k}}$ (defined from $\hat{A}_{\mathbf{k}}$ and $\hat{B}_{\mathbf{k}}$ via Equation 2.17) have bounded, discrete and linearly-spaced spectra which are given by

$$\text{Spec}(\hat{Q}_{\mathbf{k}}) = \{-\ell_{\mathbf{k}}\alpha_{\mathbf{k}}, \dots, \ell_{\mathbf{k}}\alpha_{\mathbf{k}}\}; \quad \text{Spec}(\hat{P}_{\mathbf{k}}) = \{-\ell_{\mathbf{k}}\beta_{\mathbf{k}}, \dots, \ell_{\mathbf{k}}\beta_{\mathbf{k}}\}, \quad (2.21)$$

i.e. the eigenvalue spacings of the two operators are given by $\alpha_{\mathbf{k}}$ and $\beta_{\mathbf{k}}$ respectively. It can be shown that in the limit $d_{\mathbf{k}} \rightarrow \infty$ the commutator of $\hat{Q}_{\mathbf{k}}$ and $\hat{P}_{\mathbf{k}}$ indeed approaches the infinite-dimensional CCR [42].

We would now like to quantize the Hamiltonian of Equation 2.8 in terms of these finite-dimensional operators. Taking into account the re-scaling from Equation 2.16, the Hamiltonian operator becomes

$$\hat{H} = \sum_{|\mathbf{k}| < a\Lambda_{\text{UV}}} \left[\frac{\hat{P}_{\mathbf{k}}^2}{2a^3L_c} + \frac{a^3L_c(|\mathbf{k}|^2/a^2 + m^2)}{2}\hat{Q}_{\mathbf{k}}^2 \right] \equiv \sum_{|\mathbf{k}| < a\Lambda_{\text{UV}}} \left[\frac{\hat{P}_{\mathbf{k}}^2}{2M} + \frac{M\Omega_{\mathbf{k}}^2}{2}\hat{Q}_{\mathbf{k}}^2 \right], \quad (2.22)$$

where we have defined $M = a^3L_c$ and $\Omega_{\mathbf{k}} = \sqrt{|\mathbf{k}|^2/a^2 + m^2}$ to make each individual mode formally resemble a standard quantum harmonic oscillator with time dependent mass M and time dependent frequency $\Omega_{\mathbf{k}}$. To determine the energy spectrum of this finite-dimensional constructions, we need to fix two ingredients: the dimension $d_{\mathbf{k}}$ of the Hilbert space of each

mode \mathbf{k} , and the spacing $\alpha_{\mathbf{k}}$ of the eigenvalues of $\hat{Q}_{\mathbf{k}}$ (which via Equation 2.19 also fixes the eigenvalue spacing of $\hat{P}_{\mathbf{k}}$).

As a proof of concept, [42] have considered the situation where $\alpha_{\mathbf{k}} = \beta_{\mathbf{k}} = (2\pi/d_{\mathbf{k}})^{1/2}$. We investigate the impact of that choice on the vacuum energy of our scalar field in Section 4.2, but for our fiducial construction, we opt for a different approach to selecting $\alpha_{\mathbf{k}}$ and $\beta_{\mathbf{k}}$. Recall that because of Equation 2.19 any choice of $\alpha_{\mathbf{k}}$ already fixes $\beta_{\mathbf{k}}$. Hence, for any given values of $d_{\mathbf{k}}$, $\Omega_{\mathbf{k}}$ and M , the minimum energy $E_{\min,\mathbf{k}}$ of the mode \mathbf{k} only depends on $\alpha_{\mathbf{k}}$. Now to fix a choice of $\alpha_{\mathbf{k}}$, consider the time $t_{\mathbf{k}}$ when the mode \mathbf{k} enters the sum of Equation 2.22, that is, when $|\mathbf{k}| = a(t_{\mathbf{k}})\Lambda_{\text{UV}}$. This is the time when the mode \mathbf{k} is initialized, and we are going to choose $\alpha_{\mathbf{k}}$ such that it maximises $E_{\min,\mathbf{k}}$ at that time,

$$\frac{d}{d\alpha_{\mathbf{k}}} E_{\min,\mathbf{k}}(t_{\mathbf{k}}) = 0 . \quad (2.23)$$

As we show in Appendix A, the eigenvalue spacings that satisfy this criterion are exactly given by

$$\alpha_{\mathbf{k}} = \sqrt{\frac{2\pi}{d_{\mathbf{k}}M(t_{\mathbf{k}})\Omega_{\mathbf{k}}(t_{\mathbf{k}})}} , \quad \beta_{\mathbf{k}} = \sqrt{\frac{2\pi M(t_{\mathbf{k}})\Omega_{\mathbf{k}}(t_{\mathbf{k}})}{d_{\mathbf{k}}}} . \quad (2.24)$$

It can be shown that finite-dimensionality can only decrease $E_{\min,\mathbf{k}}$ compared to its infinite-dimensional value (cf. [42] or our Appendix B). Hence, the above choice for $\alpha_{\mathbf{k}}$ and $\beta_{\mathbf{k}}$ minimizes finite-dimensional effects on the low energy spectrum of the Hamiltonian at the time $t_{\mathbf{k}}$ when the mode \mathbf{k} is initialised. Since both M and $\Omega_{\mathbf{k}}$ are functions of time, the Hamiltonian of each mode will eventually move away from that sweet spot. But as long as the vacuum energy of our field is dominated by UV modes, for which $t_{\mathbf{k}} \approx t_{\text{today}}$, our fiducial construction can be considered as conservative wrt. finite-dimensional effects.

The eigenvalue spacings of Equation 2.24 can also be motivated from a different, but related point of view. The operators $\hat{Q}_{\mathbf{k}}$ and $\hat{P}_{\mathbf{k}}$ start to contribute to our scalar field and its conjugate momentum field at $t_{\mathbf{k}}$, i.e. at the time when the mode \mathbf{k} starts to enter the sum in Equation 2.22. Let us assume that at this moment the sub-system corresponding to mode \mathbf{k} is initialised in its instantaneous ground state which we denote by $|0(\mathbf{k}, t_{\mathbf{k}})\rangle$. We would like our construction to resemble the infinite-dimensional limit as closely as possible at that time of initialization. To achieve this, we employ a ‘‘resolution criterion:’’ we demand that the system at $t_{\mathbf{k}}$ should have the same resolution in ‘‘position’’- and ‘‘momentum’’-space, i.e.

$$\frac{\langle 0(\mathbf{k}, t_{\mathbf{k}}) | \hat{Q}_{\mathbf{k}}^2 | 0(\mathbf{k}, t_{\mathbf{k}}) \rangle}{\alpha_{\mathbf{k}}^2} = \frac{\langle 0(\mathbf{k}, t_{\mathbf{k}}) | \hat{P}_{\mathbf{k}}^2 | 0(\mathbf{k}, t_{\mathbf{k}}) \rangle}{\beta_{\mathbf{k}}^2} \quad (2.25)$$

$$\Rightarrow \frac{\langle 0(\mathbf{k}, t_{\mathbf{k}}) | \hat{Q}_{\mathbf{k}}^2 | 0(\mathbf{k}, t_{\mathbf{k}}) \rangle}{\alpha_{\mathbf{k}}^4} = \frac{\langle 0(\mathbf{k}, t_{\mathbf{k}}) | \hat{P}_{\mathbf{k}}^2 | 0(\mathbf{k}, t_{\mathbf{k}}) \rangle}{(2\pi)^2} d_{\mathbf{k}}^2$$

$$\Rightarrow \alpha_{\mathbf{k}}^4 = \frac{\langle 0(\mathbf{k}, t_{\mathbf{k}}) | \hat{Q}_{\mathbf{k}}^2 | 0(\mathbf{k}, t_{\mathbf{k}}) \rangle}{\langle 0(\mathbf{k}, t_{\mathbf{k}}) | \hat{P}_{\mathbf{k}}^2 | 0(\mathbf{k}, t_{\mathbf{k}}) \rangle} \frac{(2\pi)^2}{d_{\mathbf{k}}^2} . \quad (2.26)$$

This criterion ensures that the spread of $|0(\mathbf{k}, t_{\mathbf{k}})\rangle$ in the eigenbasis of $\hat{Q}_{\mathbf{k}}$ is equally well resolved by the eigenvalue spacing of $\hat{Q}_{\mathbf{k}}$ as the spread of $|0(\mathbf{k}, t_{\mathbf{k}})\rangle$ in the eigenbasis of $\hat{P}_{\mathbf{k}}$ by the eigenvalue spacing of $\hat{P}_{\mathbf{k}}$. If this was not case, then even a seemingly high resolution in $\hat{Q}_{\mathbf{k}}$ -space could easily be identified as deviating from infinite-dimensional behaviour in $\hat{P}_{\mathbf{k}}$ -space. This is also in line with the infinite-dimensional case where both conjugate variables are equally well resolved by construction, albeit infinitely well resolved.

To the best of our knowledge, in the finite-dimensional case, no closed form expressions for the quadratic expectation values of $\hat{Q}_{\mathbf{k}}$ and $\hat{P}_{\mathbf{k}}$ are available. We can however attempt to approximate them by the corresponding expectation values of an infinite-dimensional oscillator, which when combined with Equation 2.25, results in

$$\begin{aligned} \langle 0(\mathbf{k}, t_{\mathbf{k}}) | \hat{Q}_{\mathbf{k}}^2 | 0(\mathbf{k}, t_{\mathbf{k}}) \rangle &\approx \frac{1}{2M(t_{\mathbf{k}})\Omega_{\mathbf{k}}(t_{\mathbf{k}})}, \quad \langle 0(\mathbf{k}, t_{\mathbf{k}}) | \hat{P}_{\mathbf{k}}^2 | 0(\mathbf{k}, t_{\mathbf{k}}) \rangle \approx \frac{M(t_{\mathbf{k}})\Omega_{\mathbf{k}}(t_{\mathbf{k}})}{2} \\ \Rightarrow \alpha_{\mathbf{k}} &\approx \sqrt{\frac{2\pi}{d_{\mathbf{k}}M(t_{\mathbf{k}})\Omega_{\mathbf{k}}(t_{\mathbf{k}})}}, \quad \beta_{\mathbf{k}} \approx \sqrt{\frac{2\pi M(t_{\mathbf{k}})\Omega_{\mathbf{k}}(t_{\mathbf{k}})}{d_{\mathbf{k}}}}. \end{aligned} \quad (2.27)$$

This is indeed equivalent to Equation 2.24. We consider this as further demonstration that our construction is conservative and minimizes finite-dimensional effects.

We show in Appendix B that with the above choice for $\alpha_{\mathbf{k}}, \beta_{\mathbf{k}}$, the minimum energy eigenvalue of the finite-dimensional harmonic oscillators at any time t becomes

$$E_{\min, \mathbf{k}}(t) \approx \frac{\Omega_{\mathbf{k}}(t)}{2} \operatorname{erf} \left(\frac{\pi^{3/2} M(t_{\mathbf{k}})\Omega_{\mathbf{k}}(t_{\mathbf{k}}) d_{\mathbf{k}}}{12M(t)\Omega_{\mathbf{k}}(t)} \right), \quad (2.28)$$

which approximates the exact results of [42], making them more amenable for numerical implementation at high dimensions $d_{\mathbf{k}}$. For $M(t)\Omega_{\mathbf{k}}(t) \gg M(t_{\mathbf{k}})\Omega_{\mathbf{k}}(t_{\mathbf{k}})$ the right hand side of Equation 2.28 can significantly deviate from the infinite-dimensional result $E_{\min, \mathbf{k}} = \Omega_{\mathbf{k}}(t)/2$. The minimum eigenvalue of the total Hamiltonian is then

$$E_{\min}(t) \approx \sum_{|\mathbf{k}| < a(t)\Lambda_{\text{UV}}} \frac{\Omega_{\mathbf{k}}(t)}{2} \operatorname{erf} \left(\frac{\pi^{3/2} M(t_{\mathbf{k}})\Omega_{\mathbf{k}}(t_{\mathbf{k}}) d_{\mathbf{k}}}{12M(t)\Omega_{\mathbf{k}}(t)} \right) \quad (2.29)$$

and the corresponding vacuum energy density is

$$\begin{aligned} \epsilon_{\text{vac}}(t) &\approx \frac{1}{a(t)^3 L_c^3} \sum_{|\mathbf{k}| < a(t)\Lambda_{\text{UV}}} \frac{\Omega_{\mathbf{k}}(t)}{2} \operatorname{erf} \left(\frac{\pi^{3/2} M(t_{\mathbf{k}})\Omega_{\mathbf{k}}(t_{\mathbf{k}}) d_{\mathbf{k}}}{12M(t)\Omega_{\mathbf{k}}(t)} \right) \\ &\approx \frac{1}{a(t)^4} \int_{|\mathbf{k}| < a(t)\Lambda_{\text{UV}}} \frac{d^3 \mathbf{k}}{(2\pi)^3} \frac{\sqrt{|\mathbf{k}|^2 + m^2 a(t)^2}}{2} \operatorname{erf} \left(\frac{\pi^{3/2} M(t_{\mathbf{k}})\Omega_{\mathbf{k}}(t_{\mathbf{k}}) d_{\mathbf{k}}}{12M(t)\Omega_{\mathbf{k}}(t)} \right) \end{aligned} \quad (2.30)$$

If this integral is dominated by high $k \equiv |\mathbf{k}| \approx a\Lambda_{\text{UV}}$, and if the mass m of the field is much smaller than Λ_{UV} (as must be the case for all standard model particles), then the frequency of the modes that dominate vacuum energy is given by $\Omega_{\mathbf{k}} \approx k/a$ and we can further approximate ϵ_{vac} by

$$\begin{aligned} \epsilon_{\text{vac}}(t) &\approx \frac{1}{a(t)^4} \int_{k < a(t)\Lambda_{\text{UV}}} \frac{dk k^3}{(2\pi)^2} \operatorname{erf} \left(\frac{\pi^{3/2} M(t_{\mathbf{k}})a(t)}{12M(t)a(t_{\mathbf{k}})} d_{\mathbf{k}} \right) \\ &= \int_{k_{\text{ph}} < \Lambda_{\text{UV}}} \frac{dk_{\text{ph}} k_{\text{ph}}^3}{(2\pi)^2} \operatorname{erf} \left(\frac{\pi^{3/2} M(t_{a(t)k_{\text{ph}}})a(t)}{12M(t)a(t_{a(t)k_{\text{ph}}})} d_{a(t)k_{\text{ph}}} \right), \end{aligned} \quad (2.31)$$

where k_{ph} is now physical (as opposed to co-moving) wave number. Without the error function in the integrand of this expression, this would be the standard result for vacuum energy density

of a scalar field with a hard UV cut-off (cf. Equation 2.14). In Section 4 we will see that this modification can significantly suppress $\epsilon_{\text{vac}}(t)$ in a time-dependent way.

The final ingredient we are missing in order to evaluate the above result for $\epsilon_{\text{vac}}(t)$ is the dimension $d_{\mathbf{k}}$ of the mode Hilbert spaces. It was motivated by [11] that $d_{\mathbf{k}} \lesssim 1/\pi k^2$ should be an upper bound for this dimension, based on the requirement that the maximum energy in each mode should be smaller than the Schwarzschild energy of the Universe. They however argue that this is a rather loose bound, and furthermore, their derivation was carried out with a choice for the eigenvalue spacings $\alpha_{\mathbf{k}}, \beta_{\mathbf{k}}$ that differs from our construction. In the following, we will use an agnostic parametrisation of the form

$$d_{\mathbf{k}} = D (k/\Lambda_{\text{UV}})^{n_D} + d_{\text{min}} , \quad (2.32)$$

where we take $D > 0$ and $d_{\text{min}} = 2$ to ensure that every mode is initialised with at least the Hilbert space of a qubit. Division by the physical cut-off Λ_{UV} has been introduced to keep D a dimensionless parameter, but note that k is still co-moving wave number. Note also that Equation 2.32 should be interpreted as an approximation to what should actually be a function with discrete, integer values. In Sections 3 and 4 we investigate how different values of D and n_D impact the behaviour of our finite-dimensional field and how demanding consistency with low energy physics can constrain the $D - n_D$ space.

2.3 Choice of IR scale

In the previous subsections we have quantized our field in a box of finite physical side length $L_{\text{ph}} = aL_c$. In the following we want to interpret this length as approximating the size of the observable Universe. This is a strong simplification since we would expect any meaningful boundary of the Universe to be spherical. To account for such a spherical geometry we would in principle have to change the way we discretized the field. Instead of a decomposition in terms of Fourier modes we would e.g. need to expand the field in terms of 3D Zernicke polynomials [31]. We do not expect such a procedure to qualitatively change the results of the remainder of this paper, and we leave more rigorous investigation of field discretization to follow-up work. For now, let us simply identify L_{ph} with the radius of a spherically bounded Universe.

What should we choose this radius to be at any given time? As we argued in Section 1, our classical notion of spacetime is likely to emerge from an underlying quantum theory [9, 10, 13, 14, 18, 47], and the correct choice of L_{ph} should be informed by that emergence map. To work out this map is far beyond the scope of this work, but we can at least guess a number of candidate scales. We could e.g. choose the particle horizon

$$L_p(t) = a(t) \int_{t_i}^t \frac{dt'}{a(t')} \equiv a(t)[\eta(t) - \eta_i] , \quad (2.33)$$

which defines the volume about which an observer can have information at time t . Other natural choices would be the curvature scale

$$L_R = \frac{1}{\sqrt{R}} , \quad (2.34)$$

where R is the Ricci scalar, or the Hubble scale

$$L_H = \frac{1}{H} . \quad (2.35)$$

We could also assume that the Universe has some constant co-moving size L_c and that its physical size grows proportional to the scale factor, i.e.

$$L_a = aL_c . \quad (2.36)$$

As a proof of concept, and following [5, 11, 43], we will indeed consider that last choice, with the constant co-moving IR scale L_c given by the asymptotic, co-moving particle horizon (i.e. the co-moving particle horizon in the infinite future). In our dark energy dominated FLRW Universe, this (co-moving) horizon is indeed finite and about 4.5 times as large as today's Hubble radius.

Choosing the co-moving IR scale to be constant brings with it a number of technical conveniences. For example, it results in a constant spacing $2\pi/L_c$ of the grid we used to discretize the field, such that the sum that e.g. appears in Equation 2.22 is over sub-sets of the same set of modes \mathbf{k} at any time. This especially means that our decomposition of the total Hilbert space into individual mode Hilbert spaces is well defined and constant in time. Another advantage of a constant co-moving scale L_c is that it allows us to simplify our expression for vacuum energy density (cf. Equation 2.31) to

$$\epsilon_{\text{vac}}(t) \approx \int_{k_{\text{ph}} < \Lambda_{\text{UV}}} \frac{dk_{\text{ph}} k_{\text{ph}}^3}{(2\pi)^2} \operatorname{erf} \left(\frac{\pi^{3/2} a^2(t_{a(t)k_{\text{ph}}})}{12a^2(t)} d_{a(t)k_{\text{ph}}} \right) \quad (2.37)$$

(where we have again assumed that the mass m of the field is negligible). These are however just technical conveniences, and some aspects of our derivation will need to be revisited if L_c changes in time.

3 Increase in dimension and scaling of maximum entropy

Recall that the Hamiltonian of our field is given by

$$\hat{H} = \sum_{|\mathbf{k}| < a\Lambda_{\text{UV}}} \left[\frac{\hat{P}_{\mathbf{k}}^2}{2M} + \frac{M\Omega_{\mathbf{k}}^2}{2} \hat{Q}_{\mathbf{k}}^2 \right], \quad (3.1)$$

In an expanding universe the upper summation limit in this expression increases with time. This could e.g. be interpreted such that new modes are constantly being added to the field Hilbert space, i.e. that Hilbert space dimension itself is a function of time. To avoid such a non-intuitive situation, we instead employ the view of [5], who have modelled an expanding, constant co-moving volume \mathcal{C} as a quantum circuit consisting of a number of qubits. They assume that at any time t the overall Hilbert space of that circuit factorises as

$$\mathcal{H} = \mathcal{H}_{\text{entangled}}(t) \otimes \mathcal{H}_{\text{reservoir}}(t) \quad (3.2)$$

where $\mathcal{H}_{\text{reservoir}}(t)$ consists of all of qubits in the circuit that are not entangled with any other qubit at time t , while each qubit in $\mathcal{H}_{\text{entangled}}(t)$ is part of an entangled state. Within their framework, the entanglement of the qubits in $\mathcal{H}_{\text{entangled}}(t)$ is thought to give rise to an emergent background manifold as well as to emergent, effective quantum fields on that background (cf. [9, 10] for a more detailed investigation of this emergence). They then model the time evolution of the total Hilbert space as a sequence of quantum gates in the circuit which entangle more and more qubits of the reservoir with qubits in $\mathcal{H}_{\text{entangled}}(t)$. This leads

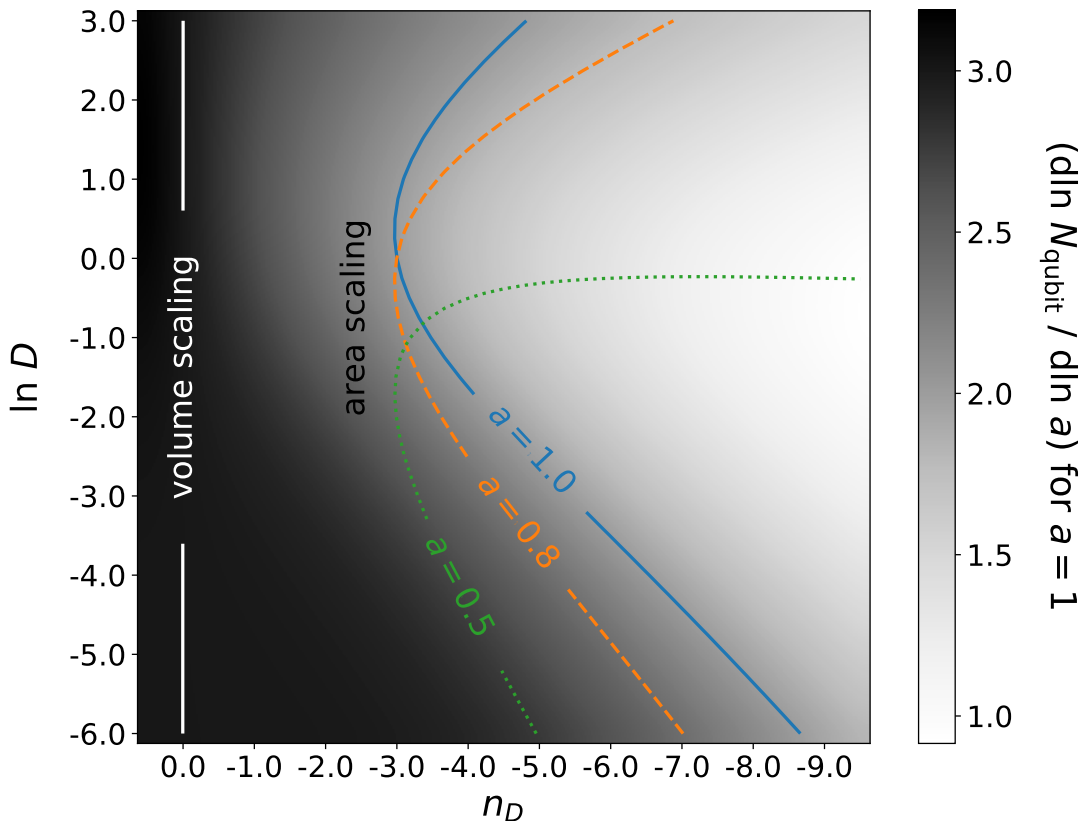


Figure 1. Color map showing how the effective number of qubits in the finite-dimensional scalar field changes with the Universe's scale factor (cf. the definition of γ_{qubit} in Equation 3.5) over a range of different values for n_D and D and for $a = 1$. The solid blue contour indicates where $\gamma_{\text{qubit}} = 2$, i.e. where N_{qubit} follows an area scaling. For any given parameter pair (n_D, D) this area scaling can only be achieved momentarily. To demonstrate this we also show the $\gamma_{\text{qubit}} = 2$ contour for $a = 0.8$ (dashed, orange line) and for $a = 0.5$ (dotted, green line).

to an increase in the dimension of $\mathcal{H}_{\text{entangled}}(t)$, which [5] in turn interpret as an increase in the physical volume of \mathcal{C} . In an attempt to connect this picture to our construction, we could conjecture that

$$\bigotimes_{|\mathbf{k}| < a\Lambda_{\text{UV}}} \mathcal{H}_{\mathbf{k}} \subset \mathcal{H}_{\text{entangled}}(t) \quad (3.3)$$

where $\mathcal{H}_{\mathbf{k}}$ are the Hilbert spaces corresponding to the individual modes \mathbf{k} , and where we consider the left hand side to be only a subset of the left hand side in order to allow for additional degrees of freedom that constitute the background geometry. From that point of view, the modes with $|\mathbf{k}| \approx a\Lambda_{\text{UV}}$ are not being newly created but they are simply carried over from the reservoir.

The effective number of qubits that are present in our field Hilbert space at any time t is given by

$$N_{\text{qubit}} = \sum_{|\mathbf{k}| < a(t)\Lambda_{\text{UV}}} \log_2(d_{\mathbf{k}}) \approx \frac{L_c^3}{(2\pi)^3} \int_{|\mathbf{k}| < a(t)\Lambda_{\text{UV}}} d^3k \log_2(d_{\mathbf{k}}). \quad (3.4)$$

Note that this number is proportional to the maximum entropy that can be attained by our field. To investigate how N_{qubit} scales with the physical size $L_{\text{ph}}(t) = a(t)L_c$, let us consider the quantity

$$\begin{aligned} \gamma_{\text{qubit}} &= \frac{d \ln N_{\text{qubit}}}{d \ln a} \\ &= 4\pi \log_2(Da^{n_D} + d_{\text{min}}) (a\Lambda_{\text{UV}})^3 \Big/ \int_{|\mathbf{k}| < a(t)\Lambda_{\text{UV}}} d^3k \log_2(d_{\mathbf{k}}) . \end{aligned} \quad (3.5)$$

If $d_{\mathbf{k}}$ was a constant function of $|\mathbf{k}|$, i.e. for $n_D = 0$, then γ_{qubit} would be equal to 3 and the maximum entropy our field would obey a volume scaling. Since the holographic principle was a motivational starting point of our analysis, we are instead interested in below-volume scaling, i.e. $\gamma_{\text{qubit}} < 3$. As we show in Figure 1, this is achieved by any $n_D < 0$. The color map in that figure shows γ_{qubit} over a range of different values for n_D and D and for $a = 1$, i.e. in today's Universe. The extend over which we plot n_D and D is motivated by Section 4, where we find that this is also the parameter range, in which the vacuum energy density of our field in today's Universe strongly deviates from a constant.

In Figure 1 we also show contours tracing the pairs (n_D, D) for which $\gamma_{\text{qubit}} = 2$, i.e. for which N_{qubit} scales as the horizon area bounding the observable Universe. Note however, that for any pair (n_D, D) such an area scaling can only be achieved momentarily. To demonstrate this, we display the area scaling contour at three different times: for $a = 1$ (solid blue), $a = 0.8$ (dashed orange) and $a = 0.5$ (dotted green). The fact that we cannot permanently achieve an area scaling seems to contradict the holographic principle. This problem may not be severe, because the scalar field modes \mathbf{k} will only constitute a small part of the overall Hilbert space (which will also include spacetime degrees of freedom, [5, 11]) and an area scaling is only expected from the total number of degrees of freedom. We nevertheless consider this a point of concern. A potential way to enforce an area scaling would be to modify the density of modes for high $|\mathbf{k}|$, as was e.g. investigated by [11] for their version of the finite-dimensional scalar field. Alternatively, it may be possible to model $d_{\mathbf{k}}$ with a functional form different from Equation 2.32 such that an exact area scaling can be achieved at all times. As long as we are ignoring spacetime degrees of freedom we are not able to motivate either of these strategies and we choose to set aside the problem for the rest of this work.

Returning to the comparison of our construction with the quantum circuit picture of [5], we can interpret the rate γ_{qubit} as the logarithmic rate in which entangling quantum gates are applied to the circuit as the Universe expands. This would constrain the way in which our Hamiltonian of Equation 3.1 is related to the Hamiltonian of the quantum circuit. The analogy between the two pictures however remains incomplete, because our construction attempts to model only a subset of all degrees of freedom that are present in the Universe. Also, both constructions are only approximate frameworks, and it is not obvious that a stringent mapping between the two should exist to begin with.

4 Equation of state of finite-dimensional vacuum energy

4.1 Fiducial construction

We had argued previously, that there are several candidate scales which could act as the physical size L_{ph} of the Universe, and that the correct choice among those scales will depend on the mapping through which the effective notion of space emerges from an underlying

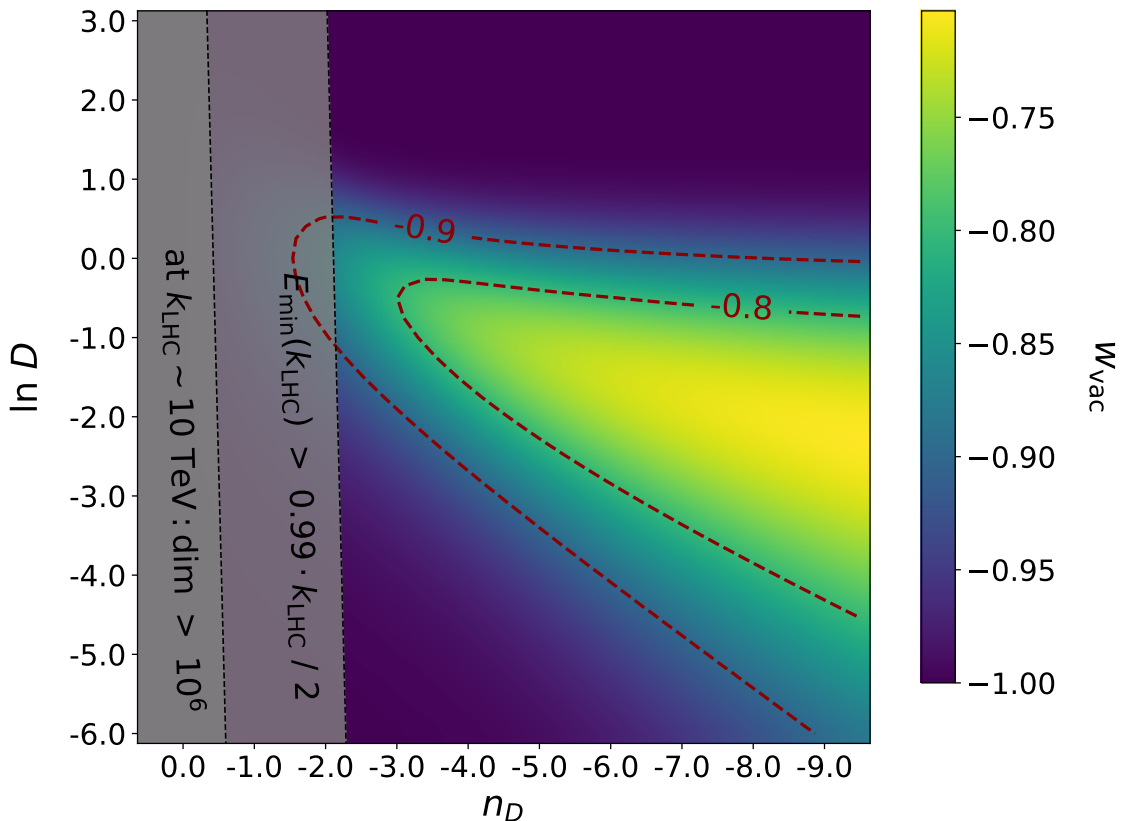


Figure 2. Color map displaying the equation-of-state parameter of the vacuum energy of our finite-dimensional scalar field as a function of the dimensionality parameters n_D and D introduced in Equation 2.32. The grey regions represent areas of parameter space we exclude in order to meet two consistency criteria: we require that on standard model scales the field be high-dimensional (left most bound; cf. discussion around (4.4)) and we require that on standard model scales the ground state energy of each wave mode is close to the infinite-dimensional limit (second to left most bound; cf. (4.5)). Both boundaries have been evaluated at a wave number $k_{\text{LHC}} \sim 10$ TeV (cf. the discussion below (4.5) for the impact of lower wave numbers on these bounds).

purely quantum theory. Working out the details of this mapping is far beyond the scope of this work, and as a proof of concept we simply assume that the Universe has a constant co-moving size L_c and that $L_{\text{ph}}(t) = L_c a(t)$, i.e. that the physical size of the Universe is proportional to the scale factor. As explained in Section 2.3, we will furthermore choose the constant co-moving IR scale L_c to be the asymptotic, co-moving particle horizon, which in our dark energy dominated FLRW Universe is about 4.5 times as large as today’s Hubble radius.

With a constant co-moving IR scale we can simplify our expression for ϵ_{vac} in Equation 2.37 even further, because the scale factor $a(t_{\mathbf{k}})$ at the time of mode entry $t_{\mathbf{k}}$ can be

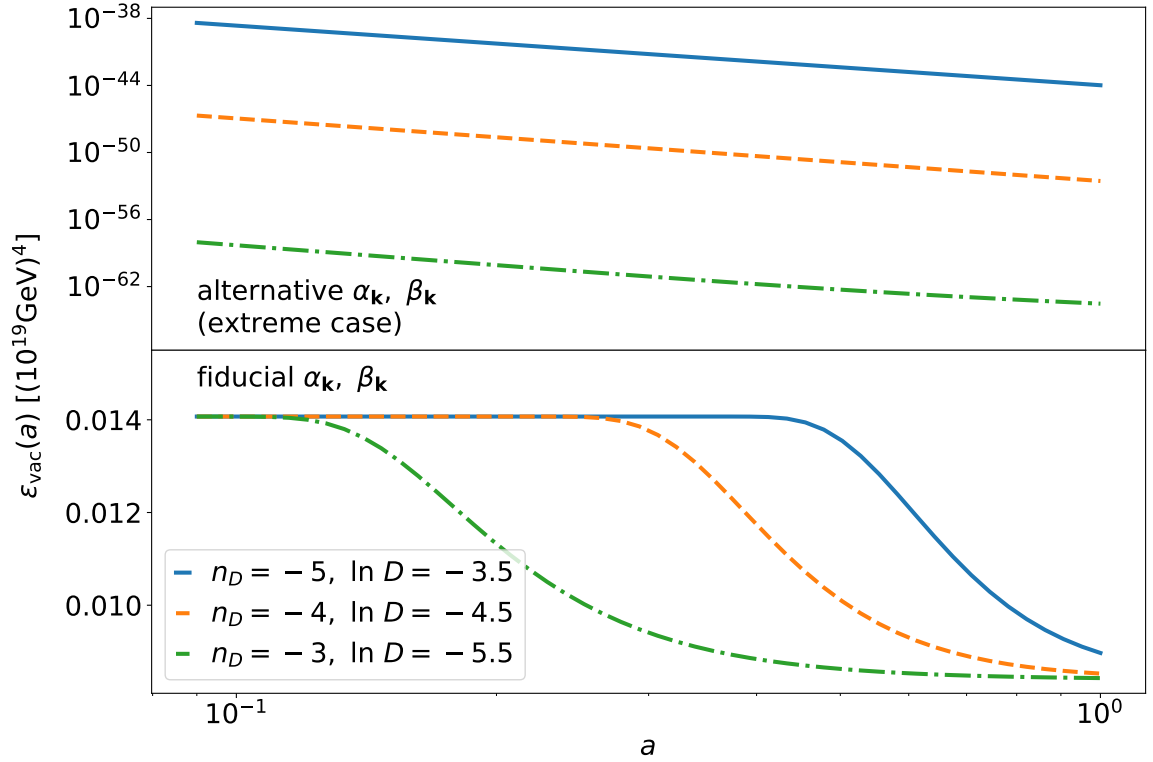


Figure 3. Evolution of vacuum energy density for different values of the dimensionality parameters n_D and D introduced in Equation 2.32. The bottom panel uses our fiducial construction with the eigenvalue spacings of the finite dimensional field operators given by Equation 2.24 while the top panel uses an extreme scenario with the eigenvalue spacings given by Equation 4.6 (cf. Section 4.2).

calculated as

$$\begin{aligned}
 k_{\text{ph}} a(t) &= k = \Lambda_{\text{UV}} a(t_{\mathbf{k}}) \\
 \Rightarrow \frac{k_{\text{ph}}}{\Lambda_{\text{UV}}} &= \frac{a(t_{\mathbf{k}})}{a(t)}. \quad (4.1)
 \end{aligned}$$

Together with our parametrization of $d_{\mathbf{k}}$ from Equation 2.32 this gives

$$\epsilon_{\text{vac}}(t) = \int_{k_{\text{ph}} \leq \Lambda_{\text{UV}}} \frac{dk_{\text{ph}} k_{\text{ph}}^3}{(2\pi)^2} \operatorname{erf} \left(\frac{\pi^{3/2}}{12} \left[\frac{k_{\text{ph}}}{\Lambda_{\text{UV}}} \right]^2 \left\{ D \left(\frac{a(t) k_{\text{ph}}}{\Lambda_{\text{UV}}} \right)^{n_D} + d_{\text{min}} \right\} \right), \quad (4.2)$$

where, as mentioned before, we take $D > 0$ and $d_{\text{min}} = 2$, such that every mode is initialised with at least the Hilbert space of a qubit. We can define an equation of state parameter $w_{\text{vac}} = w_{\text{vac}}(a)$ for this energy density through

$$\begin{aligned}
 \epsilon_{\text{vac}} &\propto \exp \left(-3 \int^a \frac{da'}{a'} (1 + w) \right) \\
 \Rightarrow w_{\text{vac}} &= - \left(1 + \frac{1}{3} \frac{d \ln \epsilon_{\text{vac}}}{d \ln a} \right). \quad (4.3)
 \end{aligned}$$

We display w_{vac} for $a = 1$ as a function of D and n_D in Figure 2. Note that the range of D and n_D over which we plot w_{vac} in that figure is the same as that of Figure 1. So the region of parameter space where w_{vac} deviates most strongly from -1 seems to roughly coincide with the region in which the maximum entropy attainable with our construction deviates most from a volume-scaling.

The space of possible values for D and n_D should be constrained by the fact that finite-dimensional effects have not been observed on standard model scales. We have implemented two qualitative versions of this constraint, which are displayed as grey regions in Figure 2. The first region results from demanding that at energies $k_{\text{LHC}} \approx 10\text{TeV}$, the dimension $d_{\mathbf{k}}$ of the individual mode Hilbert spaces be larger than some number N_{min} . This would require that

$$\begin{aligned} N_{\text{min}} &< D(k_{\text{LHC}}/\Lambda_{\text{UV}})^{n_D} + d_{\text{min}} \\ \Rightarrow \ln D &> \ln(N_{\text{min}} - d_{\text{min}}) - n_D \ln(k_{\text{LHC}}/\Lambda_{\text{UV}}) . \end{aligned} \quad (4.4)$$

It is beyond the scope of our work to determine which N_{min} would be sufficient to stay consistent with current experimental data (e.g. regarding the Higgs boson, which so far is the only scalar field of the standard model). But for the purpose of building intuition, we implement the above bound with $N_{\text{min}} = 10^6$ as the grey region to the very left of Figure 2. A second criterion we consider is the vacuum energy of modes with $k_{\text{ph}} \approx k_{\text{LHC}}$. Even for large dimensions $d_{\mathbf{k}}$, that energy can significantly deviate from the infinite-dimensional expectation $k_{\text{ph}}/2$, since it also depends on the eigenvalue spacings $\alpha_{\mathbf{k}}, \beta_{\mathbf{k}}$ as well as on the parameters M and $\Omega_{\mathbf{k}}$ appearing in the Hamiltonian in Equation 2.22. In order to ensure that finite-dimensional effects on the vacuum energy of IR scales are small we demand that

$$\text{erf} \left(\frac{\pi^{3/2}}{12} \left[\frac{k_{\text{LHC}}}{\Lambda_{\text{UV}}} \right]^2 \left[D \left(\frac{a(t)k_{\text{LHC}}}{\Lambda_{\text{UV}}} \right)^{n_D} + d_{\text{min}} \right] \right) > x , \quad (4.5)$$

where x is some number close to 1. It is again beyond the scope of this work to determine realistic values for x . But as an illustration we implement the above criterion with $x = 0.99$ as the second grey region to the left of Figure 2. Note that both Inequality 4.4 and Inequality 4.5 could be tightened further, because also many scales below k_{LHC} should be close to infinite-dimensional. E.g., for $n_D > 0$, Inequality 4.4 would always be violated if k_{LHC} was replaced by an arbitrarily small scale. Similarly, for $n_D > -2$ Inequality 4.5 could always be violated if k_{LHC} was replaced by an arbitrarily small scale. It is unclear, down to which energy scales the standard model should be expected to stay accurate [8, 19, 30], so we do not attempt to strengthen our bounds in that way.

Equation 4.2 also allows us to consider the time dependence of vacuum energy density and we follow the evolution $\epsilon_{\text{vac}}(a)$ for different values of D and n_D in the bottom panel of Figure 3. For any of the configurations (D, n_D) shown there, the vacuum energy decays between two epochs of constant energy density. Correspondingly, deviations from $w = -1$ will peak at a certain time and then fall off again. This can be understood as follows: Around the upper integration limit $k_{\text{ph}} \sim \Lambda_{\text{UV}}$ the integrand in Equation 4.2 becomes time independent both for $a \rightarrow 0$ and $a \rightarrow \infty$. So if the integral is dominated by that upper limit, then ϵ_{vac} will become time independent in both the asymptotic past and future. We discuss this further at the end of Section 4.2 where we also argue that Equation 4.2 is indeed dominated by $k_{\text{ph}} \sim \Lambda_{\text{UV}}$.

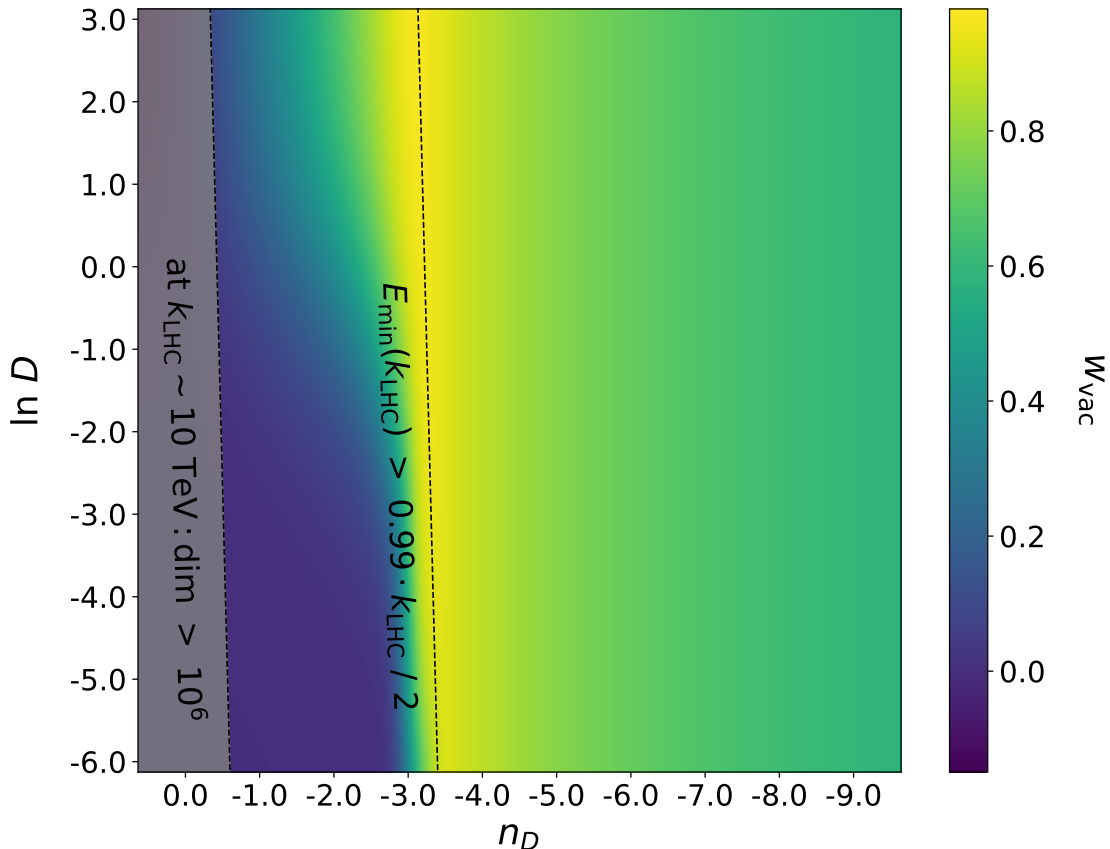


Figure 4. Same as Figure 2 but with the alternative eigenvalue spacing of the conjugate operators as given in Equation 4.6. This choice of the spacings $\alpha_{\mathbf{k}}$ and $\beta_{\mathbf{k}}$ drastically enhances finite-dimensional effects, with the equation-of-state parameter of vacuum energy reaching values up to $w_{\text{vac}} = 1$. For visual purposes we now indicate the second of our consistency criteria (requiring that standard model vacuum energy be close to infinite expressions, cf. 4.5) only as a dashed line. Note also, that the location of that boundary has changed wrt. Figure 2 because of the change in eigenvalue spacing.

4.2 Alternative choice of eigenvalue spacing

So far we had chosen the eigenvalue spacings of our finite-dimensional conjugate operators as in Equation 2.27. As we have argued around that equation (see also Appendix A) this choice is minimizing finite-dimensional effects on the low-energy spectrum of Hamiltonian $\hat{H}_{\mathbf{k}}$ of each mode \mathbf{k} at the time $t_{\mathbf{k}}$ when the mode emerges (cf. Section 3 for an interpretation of the emergence process). At the same time, vacuum energy density is dominated by the UV modes for which $t_{\mathbf{k}}$ is close to the present time. So our construction can be considered a conservative estimate of the impact of finite-dimensionality on ϵ_{vac} .

We now want to complement this estimate by an alternative choice of $\alpha_{\mathbf{k}}$ and $\beta_{\mathbf{k}}$ that leads to more drastic consequences. We can do this because we take the finite-dimensional construction as more fundamental than its infinite-dimensional limit and demand only that the former approaches the latter when actually $d_{\mathbf{k}} \rightarrow \infty$. For our alternative scenario we follow [42] in choosing

$$\alpha_{\mathbf{k}} = \sqrt{\frac{2\pi}{d_{\mathbf{k}}}} = \beta_{\mathbf{k}} . \quad (4.6)$$

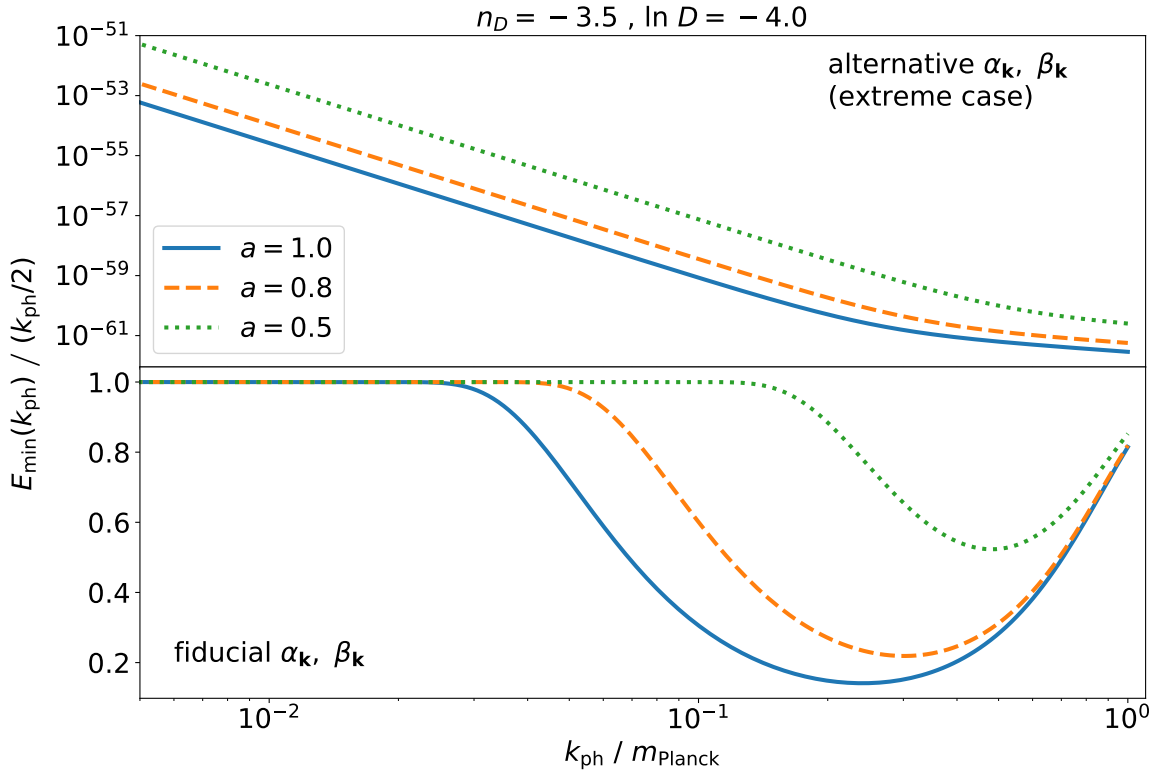


Figure 5. Showing how the error functions appearing in the integrands of Equation 4.2 (lower panel) and Equation 4.8 (upper panel) vary as a function of physical wave number k_{ph} when choosing the dimensionality parameters to be $(y, n_D) = (-4, -3.5)$ and for a number of different scale factors a . These functions encode by how much the vacuum energy of the co-moving mode $k = ak_{\text{ph}}$ is reduced with respect to the infinite-dimensional expectation of $E_{\text{min}} \approx k_{\text{ph}}/2$ in our two finite-dimensional scenarios.

These values for the eigenvalue spacings are treating both conjugate operators $\hat{Q}_{\mathbf{k}}$ and $\hat{P}_{\mathbf{k}}$ equal in an algebraic sense (though we note that $\hat{Q}_{\mathbf{k}}$ and $\hat{P}_{\mathbf{k}}$ are not uniquely determined by the infinite-dimensional limit, which was our original motivation for the resolution criterion of Equation 2.25).

As we show in Appendix B, the vacuum energy at late time of each mode \mathbf{k} with the new eigenvalue spacings is given by

$$E_{\text{min},\mathbf{k}}(t) \approx \frac{\Omega_{\mathbf{k}}(t)}{2} \operatorname{erf} \left(\frac{\pi^{3/2}}{12M(t)\Omega_{\mathbf{k}}(t)} d_{\mathbf{k}} \right), \quad (4.7)$$

where as before $M = a^3 L_c$ and $\Omega_{\mathbf{k}} = \sqrt{|\mathbf{k}|^2/a^2 + m^2} \approx |\mathbf{k}|/a$. Hence, the vacuum energy density now becomes

$$\epsilon_{\text{vac}}(t) = \int_{k_{\text{ph}} \leq \Lambda_{\text{UV}}} \frac{dk_{\text{ph}} k_{\text{ph}}^3}{(2\pi)^2} \operatorname{erf} \left(\frac{\pi^{3/2}}{12a(t)^3 k_{\text{ph}} L_c} \left[D \left(\frac{a(t)k_{\text{ph}}}{\Lambda_{\text{UV}}} \right)^{n_D} + d_{\text{min}} \right] \right). \quad (4.8)$$

The top panel of Figure 3 displays ϵ_{vac} as a function of the scale factor a for the same values of D and n_D as we had previously considered for our fiducial construction. And Figure 4

shows the equation of state parameter corresponding to the alternative expression for ϵ_{vac} as a function of D and n_D . The behaviour of vacuum energy is now radically altered compared to our fiducial construction (cf. Figure 2). Now, in most parts of parameter space, ϵ_{vac} does not act as a dark energy at all and instead rapidly decays with $w_{\text{vac}} \geq 0$.

To understand this strongly different behaviour, let us compare the error functions appearing in the integrands of Equation 4.2 and Equation 4.8. As functions of physical wave number k_{ph} they encode the amount by which the vacuum energy of the co-moving mode $k = ak_{\text{ph}}$ is reduced with respect to the infinite-dimensional expectation of $E_{\text{min}} \approx k_{\text{ph}}/2$ in our two scenarios. In our alternative scenario (i.e. the one of Equation 4.8), the error function can be approximated in terms of a piece wise power law as

$$\text{erf} \left(\frac{\pi^{3/2} \left[D \left(\frac{ak_{\text{ph}}}{\Lambda_{\text{UV}}} \right)^{n_D} + d_{\text{min}} \right]}{12a^3 k_{\text{ph}} L_c} \right) \propto \begin{cases} 1 & \text{for } D \left(\frac{ak_{\text{ph}}}{\Lambda_{\text{UV}}} \right)^{n_D} \gg k_{\text{ph}} L_c \\ (k_{\text{ph}})^{n_D-1} & \text{for } k_{\text{ph}} L_c \gg D \left(\frac{ak_{\text{ph}}}{\Lambda_{\text{UV}}} \right)^{n_D} \gg d_{\text{min}} \\ (k_{\text{ph}})^{-1} & \text{for } d_{\text{min}} \gg D \left(\frac{ak_{\text{ph}}}{\Lambda_{\text{UV}}} \right)^{n_D} \end{cases} . \quad (4.9)$$

For $n_D = -3.5$, $y = -4.0$ (a point in parameter space which results in a particularly high w in our alternative construction) and at a scale factor of $a = 1$ we demonstrate this behaviour in Appendix C (cf. Figure 7 there). We also display the above error function for a number of different scale factors ($a = 0.5$, 0.8 , 1.0) and on a reduced k_{ph} -range in the upper panel of Figure 5. For negative values of n_D these scalings imply that deviations from the infinite-dimensional vacuum energy are monotonically increasing with k_{ph} (i.e. the error function is monotonically decreasing, cf. Figure 5) when choosing our alternative spacings for the eigenvalues of the conjugate operators. The wave number above which the error function starts to noticeably deviate from 1 is approximately given by

$$k_{\text{ph}}^* \approx \left(\frac{Da^{n_D}}{(\Lambda_{\text{UV}})^{n_D} L_c} \right)^{\frac{1}{1-n_D}} . \quad (4.10)$$

This can be seen as a threshold above which modes start to contribute significantly less to the vacuum energy density of the field than they would in the infinite-dimensional case. For negative n_D that threshold is decreasing as $a(t)$ increases, which explains the strongly decaying behaviour of vacuum energy density for the alternative eigenvalue spacings of Equation 4.6.

The error function of our fiducial construction behaves quite differently. Because of an additional factor of k_{ph}^3 in its argument, it follows a piece wise scaling of

$$\text{erf} \left(\frac{\pi^{\frac{3}{2}} k_{\text{ph}}^2 \left[D \left(\frac{ak_{\text{ph}}}{\Lambda_{\text{UV}}} \right)^{n_D} + d_{\text{min}} \right]}{12\Lambda_{\text{UV}}^2} \right) \propto \begin{cases} 1 & \text{for } \left(\frac{\Lambda_{\text{UV}}}{k_{\text{ph}}} \right)^{2-n_D} \gg Da^{n_D} \\ (k_{\text{ph}})^{n_D+2} & \text{for } \left(\frac{k_{\text{ph}}}{\Lambda_{\text{UV}}} \right)^2 \gg D \left(\frac{ak_{\text{ph}}}{\Lambda_{\text{UV}}} \right)^{n_D} \gg d_{\text{min}} \\ \text{erf} \left(\frac{\pi^{\frac{3}{2}} d_{\text{min}} k_{\text{ph}}^2}{12\Lambda_{\text{UV}}^2} \right) & \text{for } d_{\text{min}} \gg D \left(\frac{ak_{\text{ph}}}{\Lambda_{\text{UV}}} \right)^{n_D} \end{cases} . \quad (4.11)$$

At least for $n_D < -2$ this implies a non-monotonic behaviour: deviations from the infinite-dimensional limit first increase with k_{ph} and then decrease again (i.e. the error function

decreases and then increases again, cf. lower panel of Figure 5). And for any n_D the error function at $k_{\text{ph}} \sim \Lambda_{\text{UV}}$ in Equation 4.2 will behave as

$$\sim \text{erf} \left(\frac{\pi^{\frac{3}{2}} [Da^{n_D} + d_{\text{min}}]}{12} \right),$$

which is always $\sim \mathcal{O}(1)$. As a consequence, the integral in Equation 4.2 is always dominated by the UV. The resulting vacuum energy is then transitioning between two dark-energy-like regimes, as discussed at the end of Section 4.1: a regime when the error function equals 1 over almost the entire integration range (which happens for $a \rightarrow 0$ as long as n_D is negative) and a regime where the UV part of the integrand has approached the limit $\sim \text{erf}(\pi^{\frac{3}{2}} d_{\text{min}}/12)$ (which happens for $a \rightarrow \infty$ as long as n_D is negative).

The stark difference between the behaviour of vacuum energy in our fiducial and in our alternative construction highlights, that effects of finite-dimensionality are highly sensitive to the details of how quantum field theory emerges from a finite-dimensional quantum theory. Neither the fiducial construction (which minimizes the impact of finite-dimensionality) nor the alternative construction (which attempts to treat both conjugate variables as algebraically equal) are likely to fully capture this emergence. In the following section we summarize the assumptions and limitations behind both scenarios and give an outlook on potential extensions and improvements.

5 Summary of assumptions and discussion

Starting from the point of view that the overall Hilbert space of the (observable) Universe should be finite, we have extended the framework of [11, 42] for describing scalar quantum fields in finite Hilbert spaces. The main ingredients of this formalism are the dimensions $d_{\mathbf{k}}$ of the individual mode Hilbert spaces $\mathcal{H}_{\mathbf{k}}$ as well as the eigenvalue spacings $\alpha_{\mathbf{k}}$ and $\beta_{\mathbf{k}}$ of the finite-dimensional conjugate field operators $\hat{Q}_{\mathbf{k}}$ and $\hat{P}_{\mathbf{k}}$ (which were defined through Equations 2.16 and 2.4). We have proposed a simple parametric ansatz to model the dependence of $d_{\mathbf{k}}$ on $|\mathbf{k}|$, and we argued that the number of degrees of freedom present in our field changes with the Universe's size with a sub-volume scaling as long as $d_{\mathbf{k}}$ is a decreasing function of $|\mathbf{k}|$ (and can momentarily even display an area-scaling). For our fiducial construction, we choose $\alpha_{\mathbf{k}}$ and $\beta_{\mathbf{k}}$ such that it minimizes the impact of finite-dimensionality on the ground state energy of the mode \mathbf{k} at the moment when the mode is initialized. We furthermore show this choice is closely tied to the requirement that both conjugate operators are equally well resolved in the ground state, making it resemble the infinite-dimensional limit as closely as possible at the time of initialization. We have then devised accurate and numerically feasible formulae of that vacuum energy as a function of $|\mathbf{k}|$, which approximate the exact calculations of [42]. With these formulae we were able to study how the vacuum energy density of our finite-dimensional scalar field depends of the dimensionality function $d_{\mathbf{k}}$. For our fiducial choice of $\alpha_{\mathbf{k}}$ and $\beta_{\mathbf{k}}$ - which minimizes finite-dimensional effects - it is decaying between two constant epochs with an overall suppression of vacuum energy by about 40%. And in an alternative construction, the equation of state parameter can even become > 0 , hence causing a rapid decay that easily suppresses vacuum energy density by $\sim 10^{-60}$ compared to the infinite dimensional result (with sharp UV cut-off) for some parameter values. We have implemented the above framework within the `GPUUniverse` toolkit that is publicly available at <https://github.com/OliverFHD/GPUUniverse>.

The finite-dimensional construction we have presented in this paper depends on the following non-trivial assumptions and modelling choices:

- We have quantized our field in a finite box, whereas any meaningful boundary of the observable Universe would be expected to be close to spherical (cf. the discussion in Section 2.3). Furthermore, our derivations have assumed that there is no spatial curvature.
- We have assumed that the Universe is of a constant co-moving size and we have chosen its radius to be the asymptotic future particle horizon (which has a finite co-moving size in a dark energy dominated universe).
- We have assumed that at any time only wave modes below a constant physical scale Λ_{UV} contribute to the field. This may be scrutinized both because we assume a sharp cut-off and because we take that cut-off to be constant in time.
- We made the assumption that it is the co-moving modes of the field that should be replaced by finite-dimensional operators. This, together with our assumption of a constant co-moving size of the Universe, means that the spacing of our grid in \mathbf{k} -space is constant in time. As a result, our factorisation of Hilbert space into mode sub-spaces $\mathcal{H}_{\mathbf{k}}$ is constant in time. This is part of a general theme of our construction: we tried to decompose our field into algebraic structures that stay constant in time.
- We chose to base our construction on generalised Pauli operators. These are able to mimic the concept of conjugate operator pairs, which according to [15] play a central role in the emergence of quasi-classical Hilbert space factorisations. But we have not investigated whether the GPO construction is the only way to achieve this dualism in finite dimensions, nor would we expect the emergent pointer observables of [15] to be given in terms of exact GPOs.
- To identify the version of the infinite-dimensional field operators which we want to replace with GPOs, we re-arranged the scalar field Hamiltonian such that it resembles the Hamiltonian of a set of harmonic oscillators.
- We only considered two different choices for the spectral spacings of the field GPOs - the ones displayed in Equation 2.25 and Equation 4.6. We tried to motivate those as representing two limiting cases: minimizing finite-dimensional effects in our fiducial choice and taking an extreme ‘quantum first’ view in our alternative choice. But an assumption common to both constructions is that we kept the spectral spacings constant in time. If the factors of Hilbert space representing different modes \mathbf{k} are indeed emergent and chosen such that they maximise a certain notion of classicality (as in the picture promoted by [15]) then one may speculate that the algebraic structures defined on these factors need to change with time in order to maintain that classicality.
- We assumed that the dimension of the mode Hilbert spaces $\mathcal{H}_{\mathbf{k}}$ as a function of $|\mathbf{k}|$ is described by Equation 2.32, i.e. that it consists of a power law in $|\mathbf{k}|$ plus a minimum dimension $d_{\min} = 2$. This assumption has allowed us to qualitatively study consistency relations for the dimensionality of our field as well as to investigate how the dimensionality function $d_{\mathbf{k}}$ impacts the way in which the number of degrees of freedom in our field changes with the expansion of the Universe. But Equation 2.32 is clearly an ad

hoc ansatz that eventually needs to be motivated or revised by an understanding of the mapping through which spacetime and effective field theories thereon arise from an underlying quantum theory.

- The maximum entropy which can be attained with our construction is still much higher than would be allowed by applying the Bekenstein bound to the entire patch of the Universe we considered. According to [11] this may require modifying the mode density function away from the three dimensional behaviour $d^3k \sim k^2 dk$ that is built into our model.

Furthermore, the equation of state of our field’s vacuum energy density as well as the consistency boundaries we derived on the dimensionality parameters D and n_D depend on a set of additional assumptions:

- We have assumed that each field mode \mathbf{k} is initialized in its instantaneous vacuum state at the time when $\mathbf{k} \approx a\Lambda_{UV}$ and that it evolves adiabatically after that, i.e. that it remains in the (time dependent) vacuum state. This is ignoring the fact that particle production during cosmic expansion will drive our field away from its vacuum state. We leave it for further work to investigate the role of particle production, particularly in a finite-dimensional paradigm, in earlier epochs of cosmological evolution.
- While we have studied the equation of state of our field’s vacuum energy during cosmic expansion, we have not considered this energy to be a source of that expansion. In particular, the energy density we obtained for our finite-dimensional field is still many orders of magnitude higher than the dark energy density that is needed to explain the observed accelerating expansion of our Universe [cf. 17, 41]. At the same time, it has been questioned whether quantum ground state energy indeed acts as a gravitational source [e.g. 24, 51].
- In the entire paper we have focused on the late-time Universe ($a \gtrsim 0.1$). An interesting line of future work would be to understand the role of finite-dimensional effects during inflation. As we discuss in Appendix B.2, this would require modifications to our calculations because Equation 2.28 is not valid for arbitrarily small a .

The plethora of assumptions and limitations we have outlined above demonstrates, that our framework and the language we have devised to describe finite-dimensional fields still require further development. At the same time, we think that it can be a fruitful starting point to explore the impact of finite-dimensionality of Hilbert space on cosmological physics.

Acknowledgments

©2022. We are thankful to ChunJun (Charles) Cao, Sean Carroll, Steffen Hagstotz and Cora Uhlemann for helpful comments and discussions. OF gratefully acknowledges support by the Kavli Foundation and the International Newton Trust through a Newton-Kavli-Junior Fellowship, by Churchill College Cambridge through a postdoctoral By-Fellowship and by the Ludwig-Maximilians Universität through a Karl-Schwarzschild-Fellowship. AS acknowledges the generous support of the Heising-Simons Foundation. Part of the research described in this paper was carried out at the Jet Propulsion Laboratory, California Institute of Technology, under a contract with the National Aeronautics and Space Administration. We indebted to the invaluable work of the teams of the public python packages NumPy [28], SciPy [48], mpmath [32] and Matplotlib [29].

References

- [1] E. Kh. Akhmedov. Vacuum energy and relativistic invariance. *arXiv e-prints*, pages hep-th/0204048, April 2002.
- [2] T. Banks. Cosmological Breaking of Supersymmetry? *International Journal of Modern Physics A*, 16(5):910–921, January 2001.
- [3] Tom Banks. QuantuMechanics and CosMology. Talk given at the festschrift for L. Susskind, Stanford University, May 2000, 2000.
- [4] Tom Banks. Cosmological breaking of supersymmetry? *Int. J. Mod. Phys.*, A16:910–921, 2001.
- [5] Ning Bao, ChunJun Cao, Sean M. Carroll, and Liam McAllister. Quantum Circuit Cosmology: The Expansion of the Universe Since the First Qubit. *arXiv e-prints*, page arXiv:1702.06959, February 2017.
- [6] Ning Bao, Sean M. Carroll, and Ashmeet Singh. The Hilbert space of quantum gravity is locally finite-dimensional. *International Journal of Modern Physics D*, 26(12):1743013, January 2017.
- [7] Raphael Bousso. The holographic principle. *Reviews of Modern Physics*, 74(3):825–874, August 2002.
- [8] Dmitry Budker. Low-energy tests of fundamental physics. *European Review*, 26(1):82–89, 2018.
- [9] ChunJun Cao and Sean M. Carroll. Bulk entanglement gravity without a boundary: Towards finding Einstein’s equation in Hilbert space. *Phys. Rev. D*, 97(8):086003, April 2018.
- [10] ChunJun Cao, Sean M. Carroll, and Spyridon Michalakis. Space from Hilbert space: Recovering geometry from bulk entanglement. *Phys. Rev. D*, 95(2):024031, January 2017.
- [11] Chunjun Cao, Aidan Chatwin-Davies, and Ashmeet Singh. How low can vacuum energy go when your fields are finite-dimensional? *International Journal of Modern Physics D*, 28(14):1944006, January 2019.
- [12] ChunJun Cao and Brad Lackey. Approximate Bacon-Shor code and holography. *Journal of High Energy Physics*, 2021(5):127, May 2021.
- [13] Sean M. Carroll. Reality as a Vector in Hilbert Space. *arXiv e-prints*, page arXiv:2103.09780, March 2021.
- [14] Sean M. Carroll and Ashmeet Singh. Mad-Dog Everettianism: Quantum Mechanics at Its Most Minimal. *arXiv e-prints*, page arXiv:1801.08132, January 2018.
- [15] Sean M. Carroll and Ashmeet Singh. Quantum Mereology: Factorizing Hilbert Space into Subsystems with Quasi-Classical Dynamics. *arXiv e-prints*, page arXiv:2005.12938, May 2020.
- [16] Horacio Casini, Marina Huerta, and José Alejandro Rosabal. Remarks on entanglement entropy for gauge fields. *Phys. Rev. D*, 89(8):085012, April 2014.
- [17] Planck Collaboration. Planck 2018 results. VI. Cosmological parameters. *A&A*, 641:A6, September 2020.
- [18] Jordan S. Cotler, Geoffrey R. Penington, and Daniel H. Ranard. Locality from the Spectrum. *Communications in Mathematical Physics*, 368(3):1267–1296, June 2019.
- [19] David DeMille, John M. Doyle, and Alexander O. Sushkov. Probing the frontiers of particle physics with tabletop-scale experiments. *Science*, 357(6355):990–994, 2017.
- [20] William Donnelly and Steven B. Giddings. Diffeomorphism-invariant observables and their nonlocal algebra. *Phys. Rev.*, D93(2):024030, 2016. [Erratum: *Phys. Rev. D*94,no.2,029903(2016)].
- [21] William Donnelly and Steven B. Giddings. Observables, gravitational dressing, and obstructions to locality and subsystems. *Phys. Rev.*, D94(10):104038, 2016.

- [22] Lisa Dyson, Matthew Kleban, and Leonard Susskind. Disturbing Implications of a Cosmological Constant. *Journal of High Energy Physics*, 2002(10):011, October 2002.
- [23] Willy Fischler. Taking de Sitter Seriously. Talk given at Role of Scaling Laws in Physics and Biology (Celebrating the 60th Birthday of Geoffrey West), Santa Fe, Dec., 2000.
- [24] S. A. Fulling. Remarks on positive frequency and Hamiltonians in expanding universes. *General Relativity and Gravitation*, 10(10):807–824, July 1979.
- [25] Steven B. Giddings. Hilbert space structure in quantum gravity: an algebraic perspective. *JHEP*, 12:099, 2015.
- [26] Steven B. Giddings. Quantum-first gravity. 2018.
- [27] Alberto Güijosa and David A. Lowe. New twist on the dS/CFT correspondence. *Phys. Rev. D*, 69(10):106008, May 2004.
- [28] Charles R. Harris, K. Jarrod Millman, Stéfan J. van der Walt, Ralf Gommers, Pauli Virtanen, David Cournapeau, Eric Wieser, Julian Taylor, Sebastian Berg, Nathaniel J. Smith, Robert Kern, Matti Picus, Stephan Hoyer, Marten H. van Kerkwijk, Matthew Brett, Allan Haldane, Jaime Fernández del Río, Mark Wiebe, Pearu Peterson, Pierre Gérard-Marchant, Kevin Sheppard, Tyler Reddy, Warren Weckesser, Hameer Abbasi, Christoph Gohlke, and Travis E. Oliphant. Array programming with NumPy. *Nature*, 585(7825):357–362, September 2020.
- [29] J. D. Hunter. Matplotlib: A 2d graphics environment. *Computing in Science & Engineering*, 9(3):90–95, 2007.
- [30] Joerg Jaeckel and Andreas Ringwald. The low-energy frontier of particle physics. *Annual Review of Nuclear and Particle Science*, 60(1):405–437, 2010.
- [31] Augustus J. E. M. Janssen. Generalized 3D Zernike functions for analytic construction of band-limited line-detecting wavelets. *arXiv e-prints*, page arXiv:1510.04837, October 2015.
- [32] Fredrik Johansson et al. *mpmath: a Python library for arbitrary-precision floating-point arithmetic (version 0.18)*, December 2013. <http://mpmath.org/>.
- [33] Frederick M. Kronz and Tracy A. Luper. Unitarily inequivalent representations in algebraic quantum theory. *International Journal of Theoretical Physics*, 44(8):1239–1258, Aug 2005.
- [34] Jérôme Martin. Everything you always wanted to know about the cosmological constant problem (but were afraid to ask). *Comptes Rendus Physique*, 13(6-7):566–665, July 2012.
- [35] Samir D. Mathur. Three puzzles in cosmology. *International Journal of Modern Physics D*, 29(14):2030013, January 2020.
- [36] Viatcheslav Mukhanov and Sergei Winitzki. *Introduction to Quantum Effects in Gravity*. 2007.
- [37] T. Padmanabhan. *Gravitation: Foundations and Frontiers*. Cambridge University Press, January 2010.
- [38] Maulik Parikh and Erik Verlinde. de Sitter holography with a finite number of states. *Journal of High Energy Physics*, 2005(1):054, January 2005.
- [39] Maulik Parikh and Erik Verlinde. de Sitter holography with a finite number of states. *Journal of High Energy Physics*, 2005(1):054, January 2005.
- [40] Maulik K. Parikh and Erik P. Verlinde. De Sitter holography with a finite number of states. *JHEP*, 01:054, 2005.
- [41] Adam G. Riess et al. Observational Evidence from Supernovae for an Accelerating Universe and a Cosmological Constant. *AJ*, 116(3):1009–1038, September 1998.
- [42] Ashmeet Singh and Sean M. Carroll. Modeling Position and Momentum in Finite-Dimensional Hilbert Spaces via Generalized Pauli Operators. *arXiv e-prints*, page arXiv:1806.10134, June 2018.

- [43] Ashmeet Singh and Olivier Doré. Does Quantum Physics Lead To Cosmological Inflation? *arXiv e-prints*, page arXiv:2109.03049, August 2021.
- [44] Leonard Susskind. The World as a hologram. *J. Math. Phys.*, 36:6377–6396, 1995.
- [45] Leonard Susskind. The world as a hologram. *Journal of Mathematical Physics*, 36(11):6377–6396, November 1995.
- [46] Gerard 't Hooft. Dimensional reduction in quantum gravity. In *Salamfest 1993:0284-296*, pages 0284–296, 1993.
- [47] Mark van Raamsdonk. Building up spacetime with quantum entanglement. *General Relativity and Gravitation*, 42(10):2323–2329, October 2010.
- [48] Pauli Virtanen, Ralf Gommers, Travis E. Oliphant, Matt Haberland, Tyler Reddy, David Cournapeau, Evgeni Burovski, Pearu Peterson, Warren Weckesser, Jonathan Bright, Stéfan J. van der Walt, Matthew Brett, Joshua Wilson, K. Jarrod Millman, Nikolay Mayorov, Andrew R. J. Nelson, Eric Jones, Robert Kern, Eric Larson, C J Carey, İlhan Polat, Yu Feng, Eric W. Moore, Jake VanderPlas, Denis Laxalde, Josef Perktold, Robert Cimrman, Ian Henriksen, E. A. Quintero, Charles R. Harris, Anne M. Archibald, Antônio H. Ribeiro, Fabian Pedregosa, Paul van Mulbregt, and SciPy 1.0 Contributors. SciPy 1.0: Fundamental Algorithms for Scientific Computing in Python. *Nature Methods*, 17:261–272, 2020.
- [49] H. Weyl. *The Theory of Groups and Quantum Mechanics*. Dover Books on Mathematics. Dover Publications, 1950.
- [50] Edward Witten. Quantum gravity in de Sitter space. In *Strings 2001: International Conference Mumbai, India, January 5-10, 2001*, 2001.
- [51] Yigit Yargic, Laura Sberna, and Achim Kempf. Which part of the stress-energy tensor gravitates? *Phys. Rev. D*, 101(4):043513, February 2020.

A Eigenvalue spacing that maximize vacuum energy

Consider the Hamiltonian

$$\hat{H} = \frac{\hat{P}^2}{2M} + \frac{M\Omega^2}{2}\hat{Q}^2, \quad (\text{A.1})$$

where \hat{P} and \hat{Q} are generalised Pauli operators as in [11, 42] (see also our Section 2.2). In the eigenbasis of \hat{X} this means that

$$\hat{Q} = \alpha \text{diag}(-\ell, \dots, \ell) \quad ; \quad \hat{P} = \beta \hat{S} \text{diag}(-\ell, \dots, \ell) \hat{S}^{-1}, \quad (\text{A.2})$$

where \hat{S} is Sylvester’s matrix (which corresponds to discrete Fourier transform), $d = 2\ell + 1$ is the dimension of Hilbert space and the eigenvalue spacings α and β satisfy $\alpha\beta = 2\pi/d$. Using this relation as well as the definition $\hat{L} \equiv \text{diag}(-\ell, \dots, \ell)$ the Hamiltonian becomes

$$\hat{H} = \frac{1}{\alpha^2} \frac{(2\pi)^2}{2Md^2} \hat{S} \hat{L}^2 \hat{S}^{-1} + \alpha^2 \frac{M\Omega^2}{2} \hat{L}^2. \quad (\text{A.3})$$

Since \hat{S} is unitary, the matrix $\hat{S} \hat{H} \hat{S}^{-1}$ has the same eigenvalues as \hat{H} . Furthermore, it can be shown that $\hat{S}^2 \hat{L}^2 \hat{S}^{-2} = \hat{L}^2$ [42]. From this it follows that the eigenspectrum of the Hamiltonian is invariant under the replacement

$$\alpha \rightarrow \tilde{\alpha} \quad \text{with} \quad \tilde{\alpha}^2 \frac{M\Omega^2}{2} = \frac{1}{\alpha^2} \frac{(2\pi)^2}{2Md^2}. \quad (\text{A.4})$$

This transformation has a fixpoint for which $\alpha = \tilde{\alpha}$ which is given by

$$\alpha_{\text{fix}} = \sqrt{\frac{2\pi}{M\Omega d}} \Rightarrow \beta_{\text{fix}} = \sqrt{\frac{2\pi M\Omega}{d}} . \quad (\text{A.5})$$

Because of the spectral symmetry wrt. the transformation $\alpha \rightarrow \tilde{\alpha}$ this fix point must extremize the minimum eigenvalue of \hat{H} . Since finite-dimensionality can only decrease the minimum eigenvalue of the Hamiltonian compared to the vacuum energy of an infinite-dimensional harmonic oscillator (cf. [42] or our Appendix B), it is reasonable to assume that α_{fix} and β_{fix} indeed maximise the ground state energy of \hat{H} . Hence, they would minimize finite-dimensional effects on the low-energy spectrum of the Hamiltonian. We were not able to strictly prove the nature of the extremum, but a range of numerical tests support our assumption. These tests also show that even for low dimensions d the extremum of vacuum energy lies very close to its infinite-dimensional value $\Omega/2$.

B Approximating $E_{\min}(k)$

B.1 General case asymptotics

Consider again the Hamiltonian of a finite-dimensional harmonic oscillator,

$$\hat{H} = \frac{\hat{P}^2}{2M} + \frac{M\Omega^2}{2}\hat{Q}^2 . \quad (\text{B.1})$$

Our goal in this appendix is to derive an approximation to the minimum eigenvalue of this operator as a function of M , Ω , d and α (cf. Appendix A for notation) that is numerically feasible even for large d . We had seen in Appendix A, that \hat{H} can be re-written as

$$\hat{H} = \frac{(2\pi)^2}{2Md^2\alpha^2} \left\{ \hat{S}\hat{L}^2\hat{S}^{-1} + \frac{\alpha^4 M^2 \Omega^2 d^2}{(2\pi)^2} \hat{L}^2 \right\} \equiv \frac{(2\pi)^2}{2Md^2\alpha^2} \left\{ \hat{S}\hat{L}^2\hat{S}^{-1} + X\hat{L}^2 \right\} . \quad (\text{B.2})$$

So to calculate the lowest energy level of \hat{H} we need to know the minimum eigenvalues of operators of the form $\hat{O}_X \equiv \hat{S}\hat{L}^2\hat{S}^{-1} + X\hat{L}^2$. At the fix point α_* we have derived in Appendix A the Hamiltonian becomes

$$\hat{H} = \frac{\Omega}{2} \frac{2\pi}{d} \left\{ \hat{S}\hat{L}^2\hat{S}^{-1} + \hat{L}^2 \right\} . \quad (\text{B.3})$$

At the same time, we had argued there that the fix point minimizes effects of finite-dimensionality, such that vacuum energy comes close to its infinite-dimensional limit $\Omega/2$ (numerical calculation confirms that this is true to high accuracy even for d as low as 5). From that we can conclude that

$$\lambda_{\min}(\hat{O}_{X \approx 1}) \approx \frac{d}{2\pi} . \quad (\text{B.4})$$

To understand the situation for more general values of X , let us consider the matrix elements of \hat{O}_X in the eigenbasis of \hat{Q} . They are given by [42]

$$[\hat{O}_X]_{ij} = \frac{1}{4} \sum_{n \neq i, j} \frac{1}{\sin\left(\frac{2\pi\ell}{2\ell+1}(n-i)\right) \sin\left(\frac{2\pi\ell}{2\ell+1}(n-j)\right)} + Xj^2\delta_{ij} , \quad (\text{B.5})$$

where all integers run from $-\ell$ to ℓ (and $d = 2\ell + 1$ as in Appendix A). In the limit $X \rightarrow \infty$ the second term in the above bracket dominates such that the eigenvector \mathbf{v} of \hat{O}_X with the lowest eigenvalue becomes

$$[\mathbf{v}]_i \propto \begin{cases} 1 & \text{for } i = 0 \\ 0 & \text{else} \end{cases} \quad (\text{B.6})$$

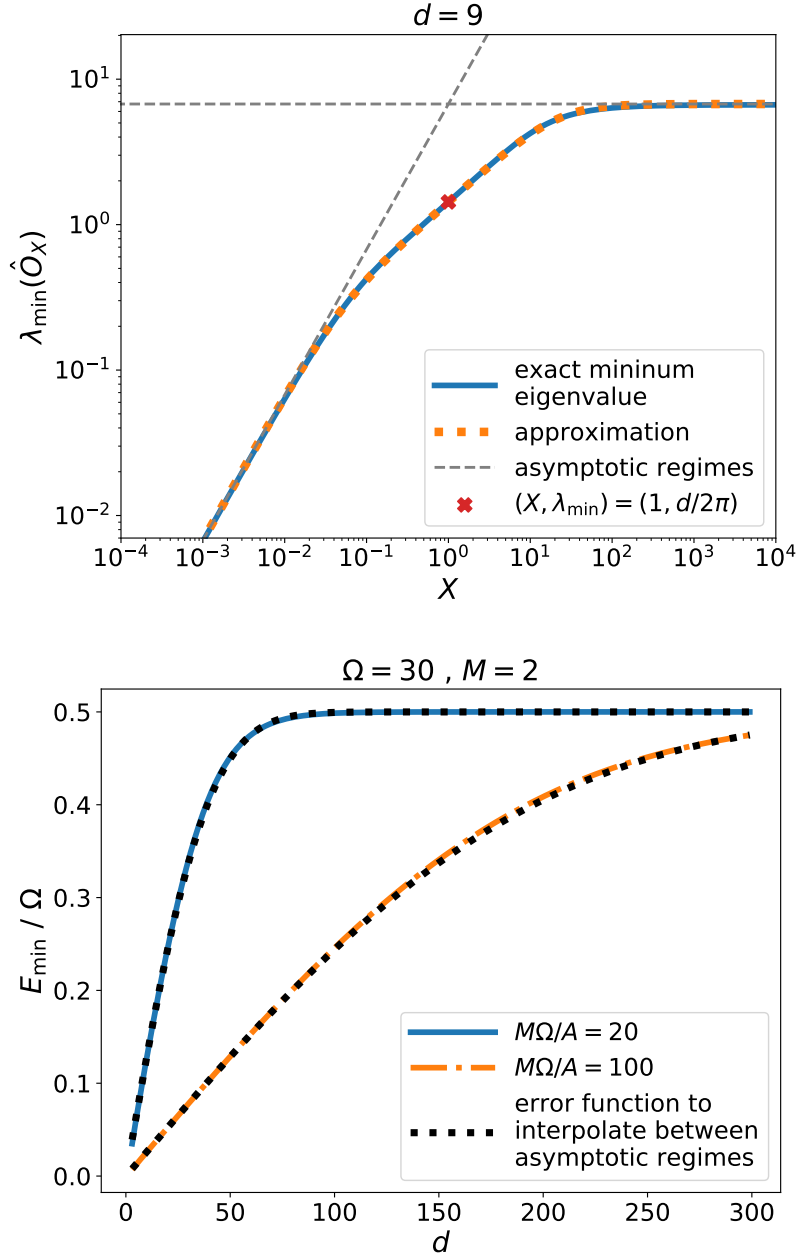


Figure 6. Upper panel: minimum eigenvalue of the operator $\hat{O}_X = \hat{S}\hat{L}^2\hat{S}^{-1} + X\hat{L}^2$ in $d = 21$ dimensions as a function of X . The blue solid line represents an exact calculation while the orange dotted line shows the approximation provided in Equation B.10. The grey dashed lines and the red cross indicate the three asymptotic regimes of Equation B.9. **Lower panel:** minimum eigenvalue of the Hamiltonian of a finite-dimensional harmonic oscillator with (dimensionless) frequency $\Omega = 30$ and mass $M = 2$ as a function of Hilbert space dimension d and for two different values of the parameter A (which determines how the eigenvalue spacing α of the position operator \hat{Q} changes as a function of d , cf. Equation B.12). The blue solid line represents the exact calculation for $A = M\Omega/20$ and the orange dash-dotted line shows the exact calculation for $A = M\Omega/100$. The black dotted lines show the approximation of Equation B.16. The agreement between approximation and exact calculation is similar over a wide range of values for Ω , M and A .

with the corresponding eigenvalue

$$\lambda_{\min}(\hat{O}_X) \approx [\hat{O}_X]_{00} = \frac{1}{2} \sum_{n=1}^{\ell} \frac{1}{\sin^2\left(\frac{2\pi\ell}{2\ell+1}n\right)} = \frac{1}{2} \sum_{n=1}^{\ell} \frac{1}{\sin^2(\pi n(1-1/d))}. \quad (\text{B.7})$$

For $d \gg 1$ we can expand this in the small parameter $x \equiv 1/d$ as

$$[\hat{O}_X]_{00} \approx \frac{1}{2\pi^2 x^2} \sum_{n=1}^{\ell} \frac{1}{n^2} \approx \frac{d^2}{12}. \quad (\text{B.8})$$

This is an approximation for $\lambda_{\min}(\hat{O}_X)$ as X approaches infinity. By the symmetry arguments we had employed in Appendix A one can then show that $\lambda_{\min}(\hat{O}_X) \approx Xd^2/12$ as X approaches zero. In summary, we obtain

$$\lambda_{\min}(\hat{O}_X) \approx \begin{cases} d^2/12 & \text{as } X \rightarrow \infty \\ d/(2\pi) & \text{for } X \approx 1 \\ Xd^2/12 & \text{as } X \rightarrow 0 \end{cases}. \quad (\text{B.9})$$

These asymptotics are matched exactly by the formula

$$\lambda_{\min}(\hat{O}_X) \approx \frac{F}{(1 + X^{-3} + GX^{-3/2})^{1/3}} \quad (\text{B.10})$$

with

$$F = \frac{d^2}{12}, \quad G = \left(\frac{\pi d}{6}\right)^3 - 2. \quad (\text{B.11})$$

We compare that formula to the exact calculation of $\lambda_{\min}(\hat{O}_X)$ in the upper panel of Figure 6 - exact and approximated result agree to within $\sim 4\%$ accuracy over the entire range of X for $d \geq 7$ (and much better for most values of X). That accuracy reduces to $\sim 6\%$ for $d = 5$ and to $\sim 15\%$ for $d = 3$.

B.2 Expressions for late-time cosmology

We can obtain a more concise formula that directly approximates the minimum eigenvalue of \hat{H} for the late-time cosmological situation of Section 4. For both constructions we considered there, the eigenvalues spacing of \hat{Q} was of the form

$$\alpha = \sqrt{\frac{2\pi}{Ad}}, \quad (\text{B.12})$$

with $A = M(t_{\mathbf{k}})\Omega_{\mathbf{k}}(t_{\mathbf{k}})$ in our fiducial construction and $A = 1$ in Section 4.2. The parameter X then becomes $X = M^2\Omega^2/A^2$, which in our fiducial construction is given as a function of \mathbf{k} and t by

$$X_{\mathbf{k}}^{\text{fid}}(t) = \frac{M(t)^2\Omega(t)^2}{M(t_{\mathbf{k}})^2\Omega(t_{\mathbf{k}})^2} \approx \left(\frac{a(t)}{a(t_{\mathbf{k}})}\right)^4. \quad (\text{B.13})$$

In an expanding universe this is clearly always larger than 1. On the other hand, in our alternative construction X becomes

$$X_{\mathbf{k}}^{\text{alt}}(t) = L_c^2 a^4 k^2 = (L_c a^3 k_{\text{ph}})^2. \quad (\text{B.14})$$

In the late-time Universe, $a \sim 1$, this is greater than 1 as long as $k \gtrsim 1/L_c \approx 3.3 \cdot 10^{-34}$ eV, i.e. on all scales relevant to the vacuum energy density of our scalar field. So for the late-time expansion we have considered in this work, we are indeed fine to consider only the two asymptotics of Equation B.9 with $X \geq 1$. In that case, and taking into account the relation between \hat{H} and \hat{O}_X , the minimum energy eigenvalue will asymptotically behave as

$$\begin{aligned} \lambda_{\min}(\hat{H}) &\approx \frac{A}{2M} \cdot \begin{cases} \pi d/6 & \text{as } M\Omega/A \rightarrow \infty \\ 1 & \text{for } M\Omega/A \approx 1 \end{cases} \\ &\approx \frac{\Omega}{2} \cdot \begin{cases} \frac{\pi Ad}{6M\Omega} & \text{as } M\Omega/A \rightarrow \infty \\ 1 & \text{for } M\Omega/A \approx 1 \end{cases}. \end{aligned} \quad (\text{B.15})$$

This behaviour can be approximately matched by the ansatz

$$\lambda_{\min}(\hat{H}) \approx \frac{\Omega}{2} \operatorname{erf} \left(\frac{\pi^{3/2} Ad}{12M\Omega} \right). \quad (\text{B.16})$$

This is the approximation we used in order to derive the results of Section 4. We compare it to the exact calculation of $\lambda_{\min}(\hat{H})$ over a limited range of d in the lower panel of Figure 6. That figure only includes results for one set of values for Ω and M and for two different values for A . But we find that Equation B.16 agrees with the exact result to within $\sim 2\%$ accuracy for a wide range of values for (Ω, M, A) as long as $d \geq 7$. For $d = 5$ this reduces to $\sim 4\%$ accuracy and for $d = 3$ to $\sim 12\%$ accuracy.

Finally, we want to note that in the early Universe the third regime of Equation B.9 can indeed become relevant - at least in our alternative construction. There one would have $X < 1$ even at $k_{\text{ph}} \approx \Lambda_{\text{UV}} = 1$ as long as $a \lesssim 3.0 \cdot 10^{-21}$. So the approximation of Equation B.16 would e.g. be not appropriate to calculate the behaviour of our finite-dimensional field during inflation, and one would have to use Equation B.10 instead. Both Equation B.16, Equation B.10 and the corresponding exact calculations are all implemented within our publicly available code package `GPUUniverse`.

C Error function asymptotics, alternative construction

For $a = 1$ we repeat the upper panel of Figure 5 on a wider range of k_{ph} in Figure 7 (solid blue line in that figure). We also show that Equation 4.9 is indeed an accurate description of the asymptotic behaviour of the error function appearing in Equation 4.8 (cf. the black dashed line in Figure 7).

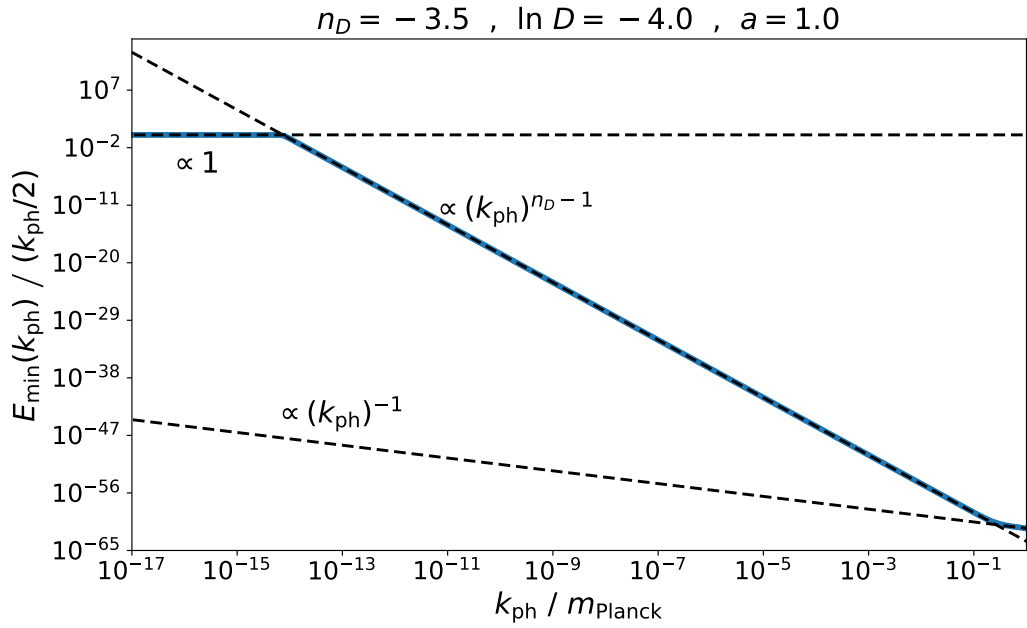


Figure 7. Displaying the upper panel of Figure 5 for $a = 1$ on a wider range of k_{ph} (solid blue line) and indicating the asymptotic behaviour stated by Equation 4.9 (black dashed lines). With the alternative eigenvalue spacings $\alpha_{\mathbf{k}}$ and $\beta_{\mathbf{k}}$ we studied in Section 4.2 (cf. Equation 4.6) the vacuum energy in each co-moving mode $\mathbf{k} = a\mathbf{k}_{\text{ph}}$ can strongly deviate from the infinite-dimensional limit $E_{\min} = k_{\text{ph}}/2$. This is in contrast to our fiducial construction where for the same parameters these deviations stay moderate even at high energy scales (cf. lower panel of Figure 5).